Geological Society of America
Special Paper 410
2006

Petrology, geochemistry, and provenance of the Galice Formation, Klamath Mountains, Oregon and California

James H. MacDonald Jr.*
Gregory D. Harper
Bin Zhu
Department of Earth and Atmospheric Sciences,
State University of New York, Albany, New York 12222, USA

ABSTRACT

The Upper Jurassic Galice Formation of the Klamath Mountains, Oregon-California, overlies the ca. 162-Ma Josephine ophiolite and the slightly younger Rogue–Chetco volcano-plutonic arc complex. The Galice Formation that overlies the Josephine ophiolite consists of a siliceous hemipelagic sequence, which grades upward into a thick turbidite sequence. Bedded hemipelagic rocks and scarce sandstone, however, also occur at several localities within the Josephine ophiolite pillow basalts. Corrected paleoflow current data suggest that the Galice Formation was derived predominantly from the east and north. Detrital modes of sandstones from the Galice Formation indicate an arc source as well as a predominantly chert-argillite source with minor metamorphic rocks. A sandstone located ~20 m below the top of the Josephine ophiolite has detrital modes and heavy mineral suites similar to the turbidite sandstones. Detrital Cr-spinel compositions from the turbidite and intra-pillow lava sandstones are also similar, indicating supra-subduction zone mantle peridotite and volcanic sources. Published detrital zircon data from a turbidite sandstone chiefly give a bimodal age distribution of 153 Ma and ca. 227 Ma but with a minor Proterozoic component. Whole-rock geochemistry from intra-pillow lava sedimentary rocks, the hemipelagic sequence, and the turbidites suggest a mixture between mafic and cratonic sources. It is suggested that the source area for the intra-pillow lava sedimentary rocks, hemipelagic sequence, and turbidites resulted from the mixing of arc and accreted terranes. These data indicate that the source areas for the Galice Formation were already established by ca. 162 Ma, probably during a Middle Jurassic orogeny that predated formation of the Josephine basin.

Keywords: Upper Jurassic, Galice Formation, hemipelagic sequence, turbidites, provenance, detrital zircons, Josephine ophiolite, California, Oregon

*Email: macdonal@atmos.albany.edu.

MacDonald, J.H., Jr., Harper, G.D., and Zhu, B., 2006, Petrology, geochemistry, and provenance of the Galice Formation, Klamath Mountains, Oregon and California, *in* Snoke, A.W., and Barnes, C.G., eds., Geological studies in the Klamath Mountains province, California and Oregon: A volume in honor of William P. Irwin: Geological Society of America Special Paper 410, p. 77–101, doi: 10.1130/2006.2410(04).

INTRODUCTION

The Upper Jurassic Galice Formation occurs within the western Klamath terrane (western Jurassic belt) of the Klamath Mountains, Oregon-California (Fig. 1). It consists predominantly of slate and lesser metasandstone, but volcanic (predominantly volcaniclastic) members are locally present. The type section of the Galice Formation conformably overlies both the ca. 160–157-Ma Rogue–Chetco volcano-plutonic arc complex and ca. 164–162-Ma Josephine ophiolite (Harper et al., 1994; Fig. 1). A lower hemipelagic sequence is present where the Galice Formation overlies the Josephine ophiolite (Fig. 2). The Galice Formation also occurs within the Elk outlier (Fig. 1), where it is in fault contact with sheeted dikes that are correlated with the Josephine ophiolite (Giaramita and Harper, this volume).

The western Klamath terrane is the youngest of a series of eastward-dipping, imbricated thrust sheets within the Klamath Mountains (Irwin, 1964, 1966, 1994; Burchfiel and Davis, 1981). The roof thrust of the western Klamath terrane, the Orleans thrust (Fig. 1), is a major crustal boundary with geological and geophysical data suggesting 40 to >100 km of displacement, respectively (Jachens et al., 1986). The basal thrust, the Madstone Cabin thrust (Fig. 1), juxtaposes the Josephine ophiolite over the Chetco intrusive complex of similar age (Dick, 1976; Harper et al., 1994; Yule, 1996). The Galice Formation is regionally metamorphosed from prehnite-pumpellyite to lower greenschist facies (Harper et al., 1988) and is unconformably overlain by Lower Cretaceous nonmarine and marine conglomerate and sandstone (Harper et al., 1994).

The Galice Formation and its basement formed in a suprasubduction setting, as indicated by the presence of the underlying Rogue–Chetco arc complex and members of similar lithology in the Galice Formation (Garcia, 1982) and a high proportion of arc detritus in metasandstones (Snoke, 1977; Harper, 1984; Wyld and Wright, 1988; Harper et al., 1994). The Galice basin apparently formed as a result of extension within a west-facing arc, ultimately resulting in seafloor spreading that produced the Josephine ophiolite (Snoke, 1977; Saleeby et al., 1982; Harper and Wright, 1984; Wyld and Wright, 1988; Harper et al., 1994; Yule et al., this volume). Seafloor spreading was postulated to have occurred in a back-arc basin behind the Rogue–Chetco arc, but the presence of boninites in the Josephine ophiolite and the apparently slightly younger age of the Rogue–Chetco arc led Harper (2004) to suggest that arc rifting and initial seafloor spreading took place in the fore-arc. Similarly, the modern Lau back-arc basin apparently first formed in the fore-arc, but became situated in the back-arc after a trenchward jump in the arc axis (Parson and Wright, 1996). Collapse of the basin occurred during the Late Jurassic Nevadan orogeny by underthrusting of the Galice Formation and its basement beneath older terranes of the Klamath Mountains, resulting in low-grade regional metamorphism (Snoke, 1977, Saleeby et al., 1982; Harper and Wright, 1984). Geochronologic and biostratigraphic data suggest that the Galice Formation was deposited

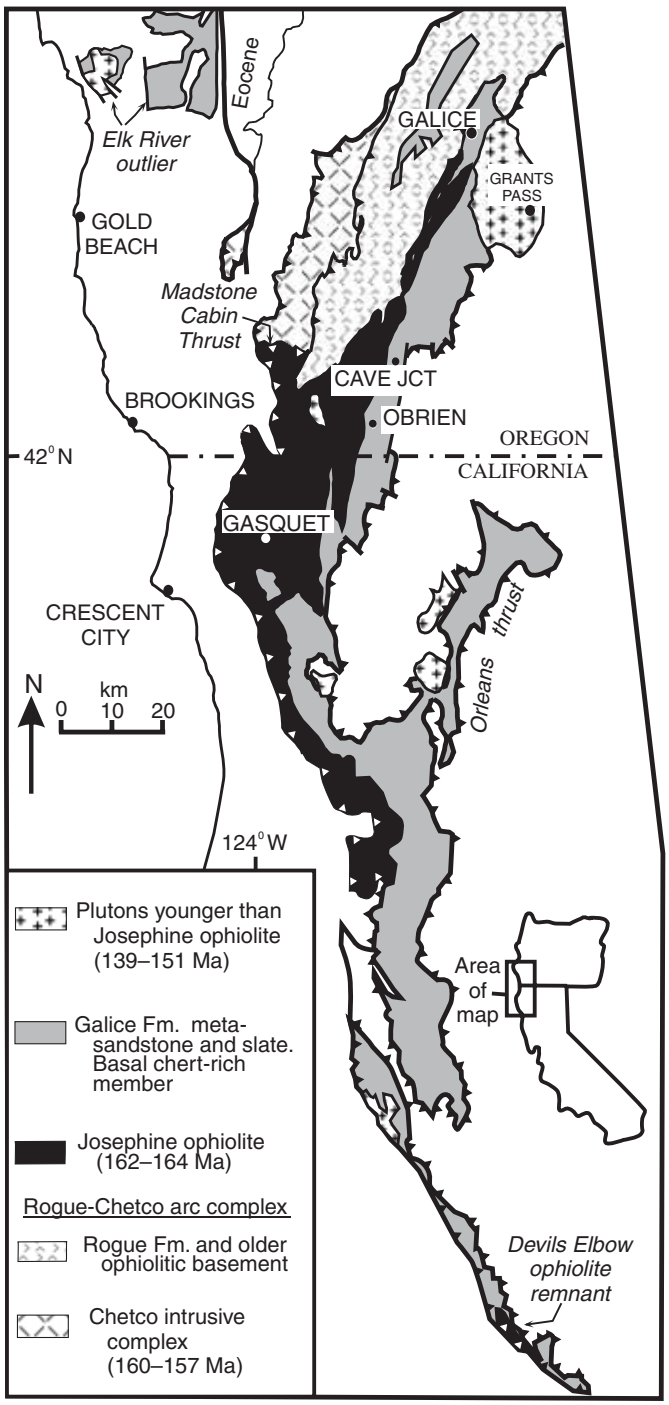

Figure 1. Generalized geologic map of western Klamath terrane, including Galice Formation. Modified from Wyld and Wright (1988), Miller and Saleeby (1995), Harper (2003), and Giaramita and Harper (this volume).

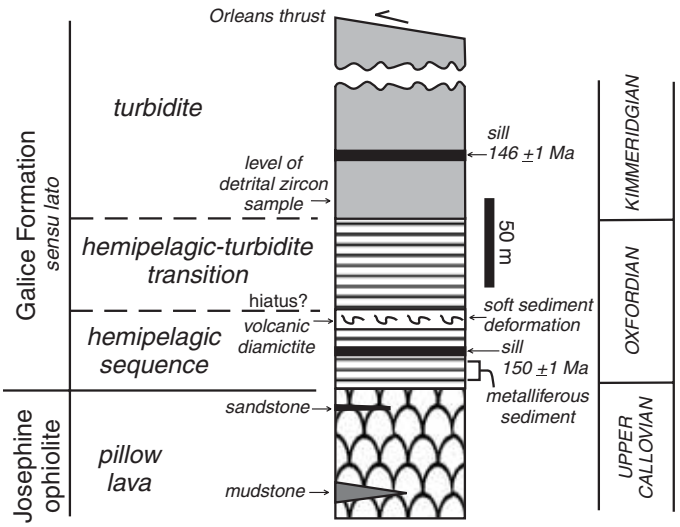

Figure 2. Sedimentary sequence overlying ca. 162-Ma Josephine ophiolite. Biostratigraphic ages are from Pessagno and Blome (1990) and Pessagno et al. (2000), and radiometric ages are from Harper et al. (1994). Location of metalliferous sediments is from Pinto-Auso and Harper (1985). Detrital-zircon sample (ca. 153- and ca. 227-Ma peaks; Miller et al., 2003) is from a locality of *Buchia concentrica* of middle Oxfordian to late Kimmeridgian age (Imlay et al., 1959). Modified from Harper (1994).

during the Nevadan orogeny, perhaps in a trenchlike basin along the western edge of the Klamath Mountains (Harper et al., 1994). The large displacement along the Orleans thrust suggests that the Josephine ophiolite was partially subducted during the Nevadan orogeny.

This chapter focuses on the provenance of the Galice Formation, based on new and existing data for detrital modes, chemistry of detrital Cr-spinel, whole-rock sedimentary geochemistry, and ages of detrital zircon. In addition, a comparison is made between the upper Galice Formation and clastic sedimentary rocks in the basal hemipelagic sequence overlying and interbedded with the Josephine ophiolite, including a newly discovered sandstone bed within the pillow lava unit.

GALICE FORMATION

Diller (1907) originally named the section of slate, sandstone, and minor conglomerate exposed on Galice Creek in southwest Oregon, west of Grants Pass, the "Galice Formation" (Fig. 1). Wells and Walker (1953) mapped the Galice 7.5-min quadrangle and recognized volcanic members lithologically similar to the underlying Rogue Formation. Cater and Wells (1953) correlated sedimentary and volcanic rocks in northern California (Gasquet 7.5-min quadrangle) with the Galice Formation, and Irwin (1960, 1966) showed the Galice Formation extending the entire length of the Klamath Mountains province. Although volcanic members are present in the type Galice Formation, Vail (1977) and Harper (1980, 1984) showed that a volcanic member mapped by Wells et al. (1949) and Cater and Wells (1953) is actually the upper part of a complete ophiolite complex (Josephine ophiolite). Volcanic members are generally absent in the Galice Formation that overlies the Josephine ophiolite (Harper, 1984), but one is present within the Galice Formation overlying the Devils Elbow remnant of the Josephine ophiolite in the southern Klamath Mountains (Wyld and Wright, 1988).

Harper (1980, 1994) suggested that the Galice Formation can be subdivided into three units (Fig. 2). The lower unit represents a hemipelagic sequence, whereas the upper unit is comprised of a turbidite sequence consisting of interbedded sandstone, siltstone, and radiolarian argillite. Lying between these two units is an ~55-m-thick transitional unit that represents the transition from hemipelagic to turbidite deposition (Fig. 2).

The ages of the Josephine ophiolite and Rogue–Chetco arc, which conformably underlie the Galice Formation, were initially thought to be the same (ca. 157 Ma; Saleeby et al., 1982; Saleeby, 1984). Based on this, Harper (1984) and Pinto-Auso and Harper (1985) included the hemipelagic sequence directly overlying the Josephine ophiolite within the Galice Formation. Subsequent biostratigraphic (Pessagno and Blome, 1990) and radiometric data (Harper et al. 1994) indicate, however, that the hemipelagic sequence is older than the type Galice Formation. This finding led Pessagno et al. (1993, 2000) to exclude the hemipelagic sequence (their "volcanopelagic succession") from the Galice Formation. Pessagno et al. (1993, 2000) suggested a hiatus occurs ~50 m stratigraphically above the Josephine ophiolite that separates the turbidite part of the Galice Formation from the underlying hemipelagic sequence (Fig. 2). They cited the much poorer preservation of radiolarians below this contact in support of their interpretation. They further suggested that the hemipelagic sequence is lithologically and genetically unrelated to the overlying turbidite; this suggestion, however, is inconsistent with petrographic and geochemical data presented below. Our observations show that bedding in rocks beneath the apparent hiatus is disrupted over a thickness of ~10 m below the hemipelagic-turbidite transition (Fig. 2). Beds are discontinuous, but not folded, and are cut by numerous small low-angle faults. This disruption appears to have occurred before complete lithification (Harper, this volume), because deformed beds and some small faults are cut by ca. 150-Ma syn-Nevadan dikes, some of which have amoeboid margins suggestive of intrusion into wet sediment (Harper, this volume).

For the purposes of this chapter, we include the hemipelagic sequence along with the turbidite in the Galice Formation (sensu lato), because the transitional unit (Fig. 2) is clearly lithologically gradational in character between the hemipelagic sequence and the Galice turbidite. Furthermore, as discussed below, sandstones in the transitional unit and in the lower part of the basal turbidite are very similar to the scarce sandstones that occur within both the hemipelagic sequence and pillow lavas of the Josephine ophiolite.

Structures in the Galice Formation that formed during the Late Jurassic Nevadan orogeny include slaty cleavage and associated overturned folds, stretching lineations, fibrous extension veins, and small thrust faults (Kays, 1968; Snoke, 1977; Harper, 1980, 1984; Norman, 1984; Gray, 1985, this volume; Wyld, 1985; Harper, this volume). The slaty cleavage and associated flattening of sand and pebble grains varies from very weak, as in the area of Cave Junction, Oregon (Jones, 1988; Fig. 1), to very strong. Strain data (i.e., Harper, 1980; Cashman, 1988; Jones, 1988) show a southward increase in strain from the Cave Junction area into northern California, coincident with an increase in metamorphic grade from prehnite-pumpellyite to lower greenschist facies (Harper, 1980; Harper et al., 1988). Paleomagnetic data suggest that the Galice Formation in southwestern Oregon may have undergone clockwise rotation of as much as 100° (Schultz and Levi, 1983; Bogen, 1986; Harper and Park, 1986).

Sedimentary Rocks within the Josephine Ophiolite

Pure, light-green chert is common between pillows in pillow lavas throughout the Josephine ophiolite. Although uncommon, bedded sedimentary rocks up to 5 m in thickness locally occur within the pillow lava unit of the Josephine ophiolite (Pinto-Auso and Harper, 1985; Kuhns and Baitis, 1987; Harper et al., 1988; Zierenberg et al., 1988; Figs. 2 and A-1). Radiolarians from these rocks indicate a late Callovian age, consistent with the ca. 162-Ma age of the Josephine ophiolite (Pessagno et al., 2000; Fig. 1). These sedimentary rocks are interbedded with Josephine lavas as well as separate mineralized lavas and massive-sulfide deposits from overlying lava flows (Pinto-Auso and Harper, 1985; Kuhns and Baitis, 1987; Zierenberg et al., 1988). Although most of the intra-pillow lava sedimentary rocks are bedded, some in the Turner-Albright mine area on the Oregon-California border southwest of Cave Junction, Oregon, are diamictites that probably formed as debris flows (Fig. A-1). These deposits and the presence of abundant talus breccias suggest the presence of fault scarps during formation of the Josephine ophiolite (Kuhns and Baitis, 1987; Zierenberg et al., 1988). The diamictites are very similar in hand sample, and in terms of geochemistry and color (black and green; Fig. A-1) to samples analyzed from the hemipelagic sequence. They are dominantly argillites, with green and black varieties interbedded on millimeter to centimeter scales. Where the regional metamorphic grade is lower-greenschist facies, they are slaty. Petrographic observations and geochemistry indicate that they are a mixture of mud, radiolarians, and hydrothermal sediment (Pinto-Auso and Harper, 1985; Kuhns and Baitis, 1987; Zierenberg et al., 1988; Figs. 2 and A-1). Less common rock types in the bedded sequences in the ophiolite include red radiolarian argillite (or slate) and chert. Detrital muscovite observed in black argillite lamella indicates a terrigenous component. The green argillite lamellae are probably tuffaceous, as shown for similar, better-studied green argillites in the hemipelagic sequence (Pinto-Auso and Harper, 1985).

An uncommon 2- to 10-cm-thick sandstone bed was found beneath the uppermost lava flow of the Josephine ophiolite, ~20 m below the depositional contact with the hemipelagic sequence in the type section of the pillow lava unit (Harper et al., 2002; MacDonald et al., 2004; Fig. 2). Harper (1994) originally identified this sandstone as a tuff, based on its characteristics in hand sample, including green color, but subsequent petrographic observations indicate the presence of terrigenous detritus, as discussed below. The green color is apparently due to ocean-ridge hydrothermal alteration, which has affected the entire pillow lava unit up to the depositional contact at this locality (Harper, 1995). Several meters along strike of where it was originally discovered, this bed has a medium-gray color similar to sandstones in the overlying Galice Formation (Harper et al., 1988).

Hemipelagic Sequence

The hemipelagic sequence is ~45-m thick and consists predominantly of green to black slaty radiolarian argillite with lesser green to black radiolarian chert (Pinto-Auso and Harper, 1985; Pessagno et al., 2000). Argillite in the hemipelagic sequence is a mixture of radiolarians, terrigenous and tuffaceous detritus, and hydrothermal sediment (Pinto-Auso and Harper, 1985; Kuhns and Baitis, 1987; Harper et al., 1988). The tuffaceous component is commonly evident from the presence of angular plagioclase, quartz (some bipyramidal; Fig. 3A) and, uncommonly, altered glass, silt, and sand (Fig. 3B). A terrigenous component from the presence of detrital muscovite is evident in thin section. The Fe/(Fe + Mn + Al) ratios indicate a relatively small metalliferous component derived from hydrothermal springs (Fig. 4), even for those overlying massive-sulfide deposits of hydrothermal origin (Kuhns and Baitis, 1987; Zierenberg et al., 1988).

Elevated metal contents are common in samples from the hemipelagic sequence, especially 8–23 m above the depositional contact with the underlying Josephine ophiolite, and some samples have sufficiently high Fe/(Fe + Mn + Al) to be classified as metalliferous (Pinto-Auso and Harper, 1985; Fig. 4). In the field, metalliferous sedimentary rocks are indicated by a shiny manganiferous coating or, less commonly, by a red color. The geochemistry and petrography of the metalliferous samples indicate that they all have substantial clastic detritus and variable amounts of radiolarians (Pinto-Auso and Harper, 1985). In addition, most of the rocks in the hemipelagic sequence, as well as those interbedded with pillow lavas of the Josephine ophiolite, have Fe/(Fe + Mn + Al) that is elevated relative to terrigenous sediments (Fig. 4), implying a small metalliferous component. Metalliferous sediments typically directly overlie ophiolites and modern ocean crust (e.g., Barrett et al., 1987). Pinto-Auso and Harper (1985) suggested that the stratigraphic

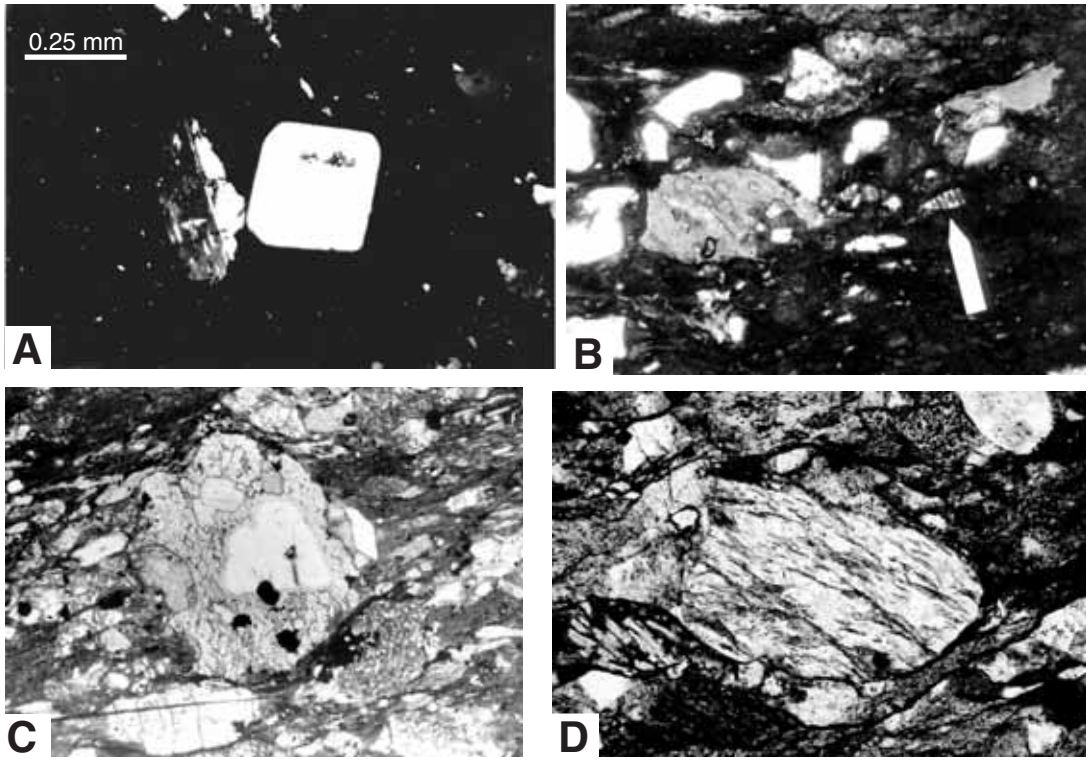

Figure 3. (A) Photomicrograph of a tuffaceous chert showing bipyramidal (volcanic) quartz and plagioclase. A 0.25-mm scale is located on figure. Crossed polarizers. (B) Photomicrograph of tuffaceous radiolarian argillite from the hemipelagic sequence showing well-preserved, cone-shaped Radiolaria (arrow), altered vesicular glass (left center), and angular quartz grains (clear). Plane light. Horizontal scale is 2 mm. (C) Photomicrograph of metasandstone from the Galice Formation showing felsic volcanic clast with resorbed quartz phenocryst. Colorless high-relief grain below this clast is augite. Note foliation in the matrix. Horizontal scale is ~1.5 mm. (D) Photomicrograph of metasandstone from the Galice Formation showing a clast of quartz-mica schist. At the lower left of this grain is a mafic volcanic clast. Dark seams are parallel to foliation. Horizontal scale is ~0.8 mm.

position of the metalliferous sediments, 8–23 m above the Josephine ophiolite, was the result of low-temperature, off-axis springs analogous to those along the flanks of the Galapagos Rise. Harper (2003) proposed that the metalliferous horizon was the result of the passage of a propagating spreading center, with the metalliferous component representing distal fallout from high-temperature, on-axis hot springs. The massive-sulfide deposits show that hydrothermal springs that could produce Fe- and Mn-rich metalliferous sediments were present during eruption of the Josephine pillow lavas. Thus, the low metal content of intra-pillow lava sedimentary rocks, including those directly overlying the massive sulfide deposits, and of sedimentary rocks comprising the lower 8 m of the hemipelagic sequence is apparently the result of dilution by abundant terrigenous mud.

Sandstone and scarce volcanic pebbly mudstone are uncommon rock types in the hemipelagic sequence (Pinto-Auso and Harper, 1985; Harper, 1994; Pessagno et al., 2000). The pebbly mudstone occurs ~40 m above the depositional contact with the Josephine ophiolite. It contains volcanic clasts up to 20 cm in diameter and has a radiolarian-tuffaceous matrix containing biotite (Harper, 1994). Sandstone was observed at two localities within the hemipelagic sequence; one within an isolated outcrop but the other ~7–8 m above the contact with the Josephine ophiolite (Pinto-Auso and Harper, 1985; Fig. 5). The sandstone beds are graded (Fig. 5) and compositionally very similar to those in the basal part of the turbidite sequence, with ~95% of the grains consisting of lithic volcanic rock fragments, plagioclase, and clinopyroxene. Other clasts, especially in the very coarse fraction, are predominantly chert and siliceous argillite. Scouring of underlying chert is evident along the base of one of these sandstone beds; this bed also contains a 3-cm angular rip-up clast of underlying chert (Fig. 5). Pessagno and Blome (1990) also reported the presence of "pelagic limestone," but these occur as nodules and probably formed by replacement of radiolarian argillite. Formation of the nodules occurred before formation of slaty cleavage (i.e., diagenetic) because radio-

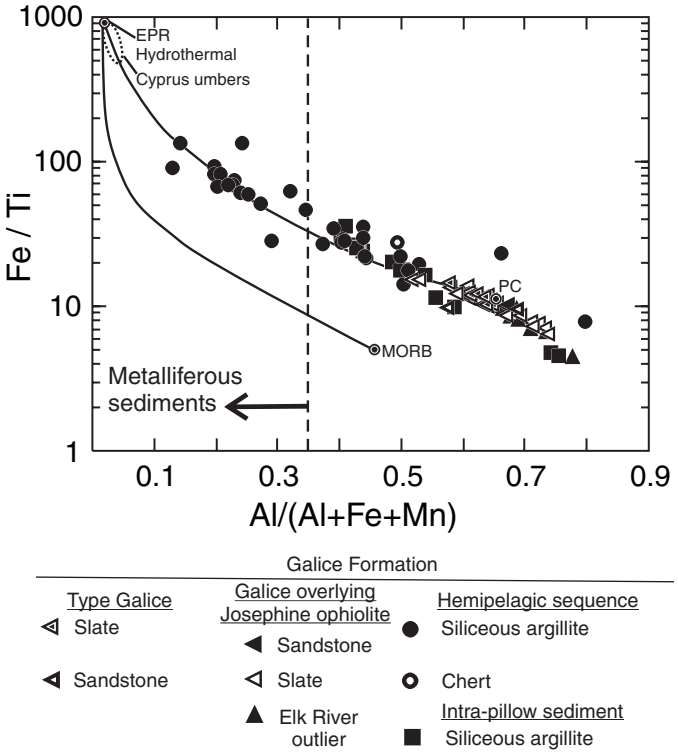

Figure 4. Plot illustrating apparent mixing relationships for sedimentary rocks within Josephine ophiolite, hemipelagic sequence, and Galice Formation. Mixing curves are for East Pacific Rise (EPR), hydrothermal sediment, and Pacific pelagic clay (PC), and EPR hydrothermal sediment and mid-ocean ridge basalt (MORB; values from Barrett, 1981). Also shown is field for Margi umbers, Cyprus, which are pure metalliferous sediment (Ravizza et al., 1999). Figure modified from Pinto-Auso and Harper (1985) and Harper et al. (1988).

larians and other spherical features (pellets?) in the nodules are undeformed.

The age range of the hemipelagic sequence is late Callovian to middle Oxfordian, according to the radiolarian biostratigraphy of Pessagno et al. (1993, 2000; Fig. 2). The absolute age range is from ca. 162 (age of the underlying ophiolite) to ca. 157 Ma. The younger age limit is based on correlation of the top of the hemipelagic sequence to radiolarian tuffs at the top of the Rogue Formation; Saleeby (1984) reports a Pb/U zircon age of 157 ± 2 Ma for volcanic rocks beneath the radiolarian tuffs, so the age of the top of the hemipelagic sequence may be somewhat less than 157 Ma. The apparently missing section at the top of the hemipelagic sequence (Fig. 2), suggested by radiolarian biostratigraphy, may be a disconformity (Pessagno and Blome, 1990). Although it may indeed be a disconformity, rocks immediately beneath the contact show considerable disruption of bedding, probably before complete lithification (Harper, this volume; Fig. 2). Thus, the apparent hiatus may be due to normal faulting or to submarine landsliding prior to deposition of the hemipelagic-turbidite transition unit.

Transition Zone

An ~55-m-thick transition zone exists between the lower hemipelagic sequence and the upper turbidite of that part of the Galice Formation that overlies the Josephine ophiolite (Harper, 1994; Fig. 2). This zone consists predominantly of radiolarian argillite with minor sandstone. The proportion of radiolarians and the proportion and size of clasts (mostly silt) are generally higher than those of radiolarian argillites in the hemipelagic sequence, and there is a negligible hydrothermal component (Pinto-Auso and Harper, 1985). Radiolarian-bearing limestone nodules occur throughout the transition zone, being abundant at the top of the zone (Harper, 1994). The lower contact for the transition zone is defined only for one section located along the Middle Fork of the Smith River, a sequence that includes the type section of the pillow lava unit of the Josephine ophiolite (Harper, 1994, 2003). In this section, which was studied by Pessagno and Blome (1990), as well as by Pinto-Auso and Harper (1985), the base of the transition zone is marked by the lowest occurrence of sandstone beds above the Josephine ophiolite.

Pessagno and Blome (1990) included rocks of the transition zone in the Galice turbidite, but we reserve use of the term "turbidite" for rocks above what we call the transition zone (Fig. 2). The above authors used the lowest occurrence of sandstones, as

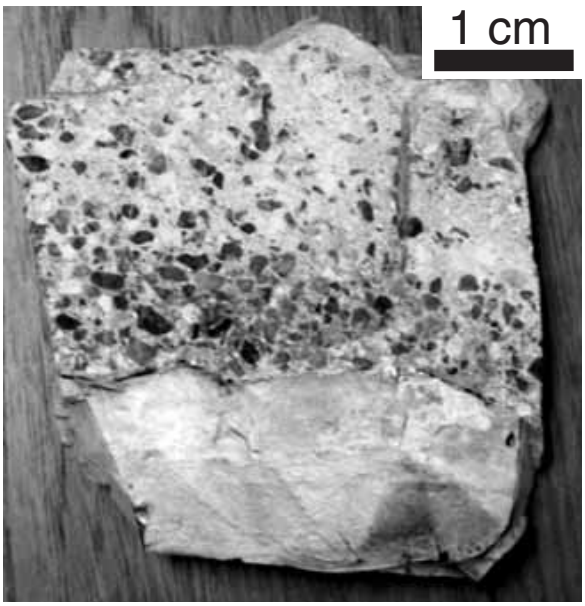

Figure 5. Graded bed from hemipelagic sequence of the Galice Formation. Bed beneath sandstone is a radiolarian chert. On the back side of this sample there is a 3-cm subangular rip-up clast of underlying sediment located within sandstone.

well as the presence of the hiatus discussed in the preceding paragraph, to define the contact between the hemipelagic sequence (their "volcanopelagic unit") and the transition zone (their "Galice Formation sensu lato"). As noted above, a sandstone bed occurs within the pillow lava unit of the ophiolite (at this locality); at other localities, sandstone beds occur within the hemipelagic sequence (Fig. 5). Thus, the use of the first sandstone beds to define the base of the transition zone in the section (Fig. 2) is only valid for this particular location. We interpret the contact to be gradational, with an upward increase in proportion of sandstone beds and decreasing proportion of radiolarians in argillites.

According to the biostratigraphy of Pessagno et al. (1993, 2000), the transition zone ranges in age from middle Oxfordian to middle Kimmeridgian. Recently, Miller et al. (2003) estimated the age of deposition of a massive sandstone from the base of the overlying turbidite sequence to be ca. 153 Ma, based on the age of the youngest detrital zircon age spectrum (Miller et al., 2003). Thus, deposition of the transition zone appears to have ranged from ca. 157 to ca. 153 Ma.

Turbidite of the Galice Formation

The base of the turbidite sequence, as defined in this chapter, occurs ~100 m above the top of the Josephine ophiolite at the locality represented in Figure 2. The Galice Formation in its type area, where it overlies the Rogue Formation, consists entirely of turbidite (i.e., no hemipelagic sequence) that interfingers with various volcanic members. The Galice turbidite consists predominantly of slate and thin-bedded to massive metasandstone, along with scarce pebble conglomerate. Sandstones are predominantly feldspathic litharenites, are commonly graded, show scouring along their bases, and display partial to complete Bouma sequences. Load and flame structures, sole marks, and mud rip-up clasts are locally common. Trace fossils from slates include *Chondrites, Cosmophorae,* and *Spirophycus,* which indicate abyssal, or perhaps bathyal, water depths (A.A. Ekdale, written commun., 1980). In the section represented in Figure 2, and extending at least 10 km farther north and 1 km farther south, a 200- to 300-m-thick massive sandstone unit overlies the transition zone between the hemipelagic and turbidite sequences (Cater and Wells, 1953; Harper, 1980). The thickness of the turbidite cannot be accurately determined, due to repetition by folding and faulting, but the original stratigraphic thickness was probably at least several kilometers, based on its large outcrop area (Fig. 1).

The Galice turbidite, in both its type area and where it overlies the Josephine ophiolite, contains the bivalve *Buchia concentrica,* which has a known age range of middle Oxfordian to late Kimmeridgian (Imlay et al., 1959; Imlay, 1980). The age of the base of the turbidite based on the biostratigraphy of Pessagno et al. (1993, 2000) is middle Kimmeridgian. The absolute age of the turbidite is constrained by the ca. 153-Ma age of the youngest detrital zircons (Miller et al., 2003) and the age of crosscutting dikes, sills, and small plutons, which are as old as ca. 150 Ma (Harper et al., 1994).

PALEOFLOW DATA

Paleoflow data were obtained by Park-Jones (1988) for the type Galice Formation overlying the Rogue Formation west of Grants Pass, Oregon, and by us for the Galice Formation overlying the Josephine ophiolite where it is exposed in Rough and Ready Creek, southwest of Cave Junction, Oregon. Folds in the Galice Formation usually are plunging, so paleoflow data were restored by first rotating the fold axis (usually bedding-cleavage intersection) to horizontal, followed by rotation of bedding to horizontal. The resulting bidirectional and unidirectional flow directions are plotted in Figure 6. Predominantly west paleocurrent directions (in present-day coordinates) were found for the type Galice Formation (Park-Jones, 1988; Fig. 6), compared to predominantly north directions for the Galice Formation overlying the Josephine ophiolite (Fig. 6). The paleocurrent data probably need to be corrected for clockwise rotation of the Klamath Mountains, which has been suggested to explain paleomagnetic declination anomalies (Mankinen and Irwin, 1982; Schultz and Levi, 1983; Bogen, 1986; Renne and Scott, 1988; Smith and Harper, 1993). Some workers (e.g., Mankinen and Irwin, 1982; Bogen, 1986) argued that the entire Klamath Mountains rotated as a single block, whereas others have argued that the arcuate shape of the Klamath Mountains is the result of oroclinal bending, possibly related to formation of the Columbia embayment (Renne and Scott, 1988; Saleeby and Harper, 1993). The strike of slaty cleavage at both localities for which there are paleocurrent data is ~020°–030° (Park-Jones, 1988; this study). Figure 6B and D show the paleocurrent data after correcting for an assumed clockwise rotation of 65°, which assumes the western Klamath terrane had an original trend of ~340°, parallel to the overall structure of correlative rocks in the Sierra Nevada foothills, which have not been rotated (Bogen et al., 1985; Frei, 1986). The inferred ~65° rotation for the Galice Formation in southwest Oregon is less than the ~100° and ~78° clockwise rotations inferred for a volcanic member in the type Galice section and for the Grants Pass pluton that intrudes the Galice Formation (Schultz and Levi, 1983; Bogen, 1986), respectively, and the ~100° for the Josephine ophiolite (Smith and Harper, 1993). The actual amount of clockwise rotation may be less than suggested by the paleomagnetic data because of unknown amounts of post-Nevadan tilting, observed in Cretaceous sedimentary rocks elsewhere in the west-central and northwest Klamath Mountains, and possibly because of insufficient magnetic cleaning (Harper and Park, 1986; Renne and Scott, 1986).

DETRITAL MODES

Sandstones within the Galice Formation are generally lithic wackes and feldspatholithic wackes (Snoke, 1977; Harper, 1980; Wyld, 1985). Sandstones are generally foliated (e.g., Fig.

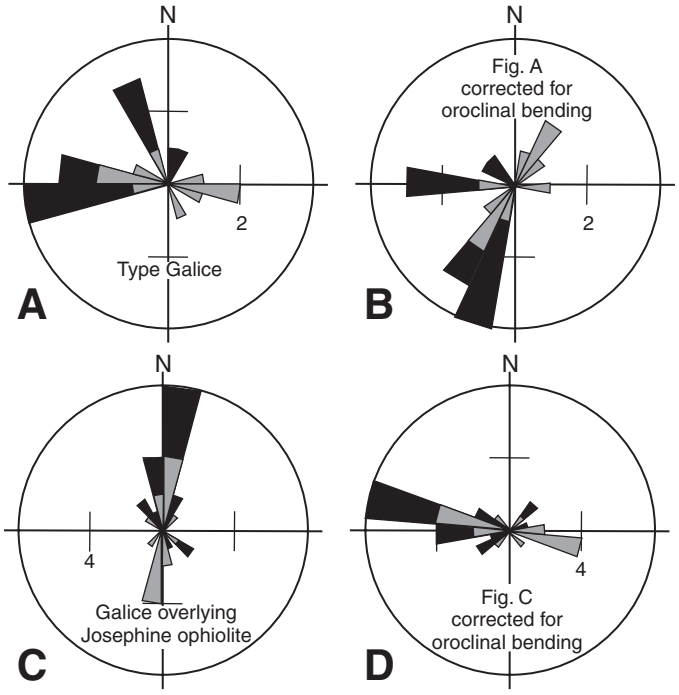

Figure 6. Rose diagrams displaying paleoflow current directions. (A) Type area of the Galice Formation, corrected for folding (from Park-Jones, 1988). (B) Type area of Galice, also corrected for inferred ~65° oroclinal bending of the Klamath Mountains. (C) Galice Formation that overlies Josephine ophiolite, corrected for folding. (D) Galice Formation that overlies Josephine ophiolite, also corrected for inferred ~65° oroclinal bending of Klamath Mountains. Unidirectional data displayed in black, bimodal data are gray. Intervals of 15° are used. Note the different scale in A and B, and C and D.

3C and D) but range from strongly foliated to unfoliated (Fig. 5), as in the Cave Junction to Obrien, Oregon, area. Clastic textures, however, are still evident in all samples. The most abundant detrital components are siliceous argillite and chert (both commonly with vestiges of radiolaria), plagioclase, and volcanic rock fragments. Less common clast types include monocrystalline and polycrystalline quartz; whereas phyllite, quartz-mica schist (Figs. 3C and D), foliated polycrystalline quartz, and siltstone or sandstone were observed with even less frequency (Snoke, 1972; Harper, 1980; Wyld, 1985). Harper (1980) and Norman (1984) determined that no K-feldspar is present in Galice sandstones that they studied, using both standard thin-section observations as well as staining. We found no K-feldspar by staining an additional thirty samples from both the type Galice Formation and the Galice Formation overlying the Josephine ophiolite near the Oregon-California border. Wyld (1985), however, reported very minor amounts (<1%) of K-feldspar in sandstones from the southernmost Klamath Mountains (Fig. 1).

Detrital modes for Galice sandstones were determined by Harper (1980), Norman (1984), and Wyld (1985). Medium- to coarse-grained sandstones were point-counted following the procedures of Dickinson (1970) and the terminology of Ingersoll and Suczek (1979) as well as Ingersoll et al. (1984). The detrital modes should be considered semiquantitative, due to partial recrystallization and, in many samples, deformation during low-grade metamorphism. Matrix generally constitutes >20%, and in some samples >30%, of the counted points. Such matrix contents are much higher than those for modern turbidites and are probably the result of alteration of lithic fragments (e.g., Dickinson, 1970, 1985). Quantitative modal analysis is also compromised by the textural similarity of many felsic volcanic rock fragments to chert; only Harper (1980) used feldspar staining to remove this uncertainty.

Structural complexity of the Galice Formation does not allow for accurate determination of stratigraphic height above basement. Harper (1980) and Wyld (1985), however, had sufficient stratigraphic control to broadly group their samples into basal, lower, and middle-upper.

Harper (1980) found that 62–92% of the volcanic rock fragments in samples of Galice sandstone have microlitic textures that are typical of andesites. Altered glass (replaced by chlorite) ranges from ~1–23% of volcanic clasts, although most samples have <10%. The proportion of felsitic clasts is highly variable, ranging from 3 to 33% of volcanic clasts. Clasts with lathwork texture (mafic) are much less common, never comprising >4% of the volcanic clasts.

The lithic- and feldspathic-rich nature of the sandstones is evident on various triangular diagrams (Fig. 7). Some sandstones plot as moderately quartz-rich on the quartz-feldspar-lithic (Q–F–L) diagram (Fig. 7A), but chert dominates the Q fraction, and monocrystalline quartz (Q_m) contents are low, as evident on the monocrystalline quartz-feldspar-lithic diagram (Q_m–F–L_t; Fig. 7B). Polycrystalline quartz (Q_p), consisting of quartz sandstone, and quartz siltstone, is generally a minor component (Fig. 7C), but abundant chert and argillite results in high values of lithic sedimentary clasts (L_{sm} in Fig. 7D; L_{sm} = sedimentary lithic + metasedimentary lithics, L_v = volcanic lithic). Detrital modes of sandstones for the Galice Formation from its type area (Harper, 1980), near the Oregon-California border (Harper, 1980; Norman, 1984), and from where it overlies the Devils Elbow remnant of the Josephine ophiolite in the southern Klamath Mountains, are similar (Fig. 7). Those samples overlying the Devils Elbow remnant, however, tend to be less rich in lithic fragments (Fig. 7A and B) and have more monocrystalline quartz (Fig. 7B).

A trend of increasing proportion of total quartz (Q; mostly chert), Q_m, Q_p, and L_{sm} (mostly siliceous argillite and chert) with increasing stratigraphic height is evident in Figure 7 for samples overlying the Devils Elbow remnant of the Josephine ophiolite in the southern Klamath Mountains (Wyld, 1985). A similar trend is evident for the Galice Formation overlying the Josephine ophiolite in its type area in northwestern California

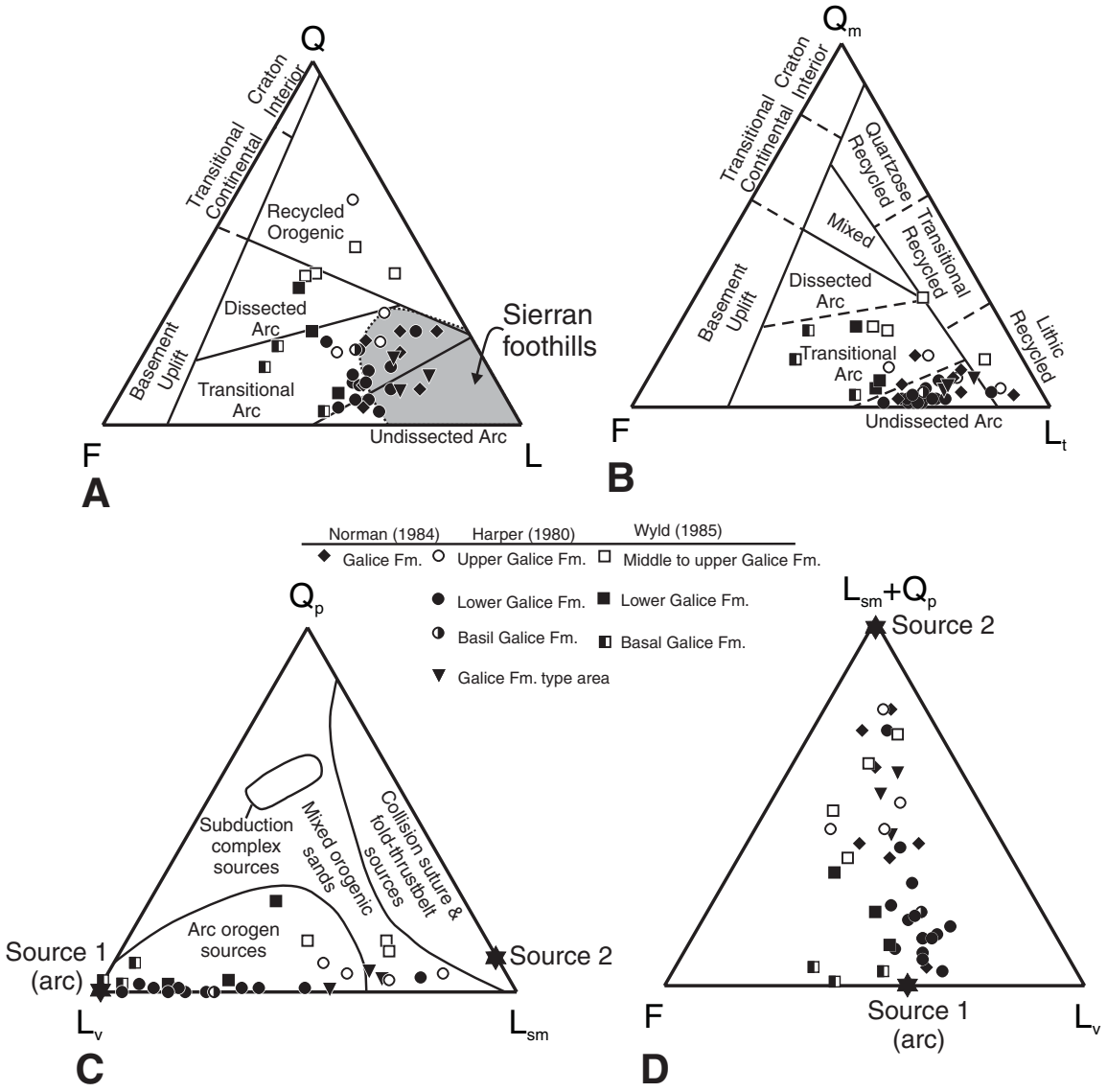

Figure 7. Triangular plots of point-count data for sandstones from Galice Formation in its type area (Harper, 1980), where it overlies the Josephine ophiolite near the Oregon-California border (Harper, 1980; Norman, 1984), and overlying Devils Elbow remnant of the Josephine ophiolite in the southern Klamath Mountains (Wyld, 1985). Q—monocrystalline quartz + polycrystalline quartz + chert; F—feldspar (all plagioclase in these samples); L—unstable lithics; Q_m—monocrystalline quartz; L_t—total polycrystalline lithic fragments, including stable quartzose; Q_p—chert + polycrystalline quartz; L_v—lithic volcanics; L_{sm}—sedimentary + metasedimentary lithics. (A) Q–F–L diagram after Dickinson et al. (1983). Shaded field is for correlative rocks in the Sierra Nevada foothills, including the Mariposa Formation (Behrman and Parkinson; 1978). (B) Q_m–F–L_t diagram after Dickinson et al. (1983). (C) Q_p–L_v–L_{sm} diagram after Dickinson (1985). Inferred end-member sources for Galice sandstones are indicated. (D) L_{sm}+Q_p–F–L_v diagram.

(Harper, 1980; Norman, 1984), except that some lower Galice sandstones have modes similar to those typical of the upper Galice (Fig. 7). This similarity is not the result of uncertainties in stratigraphic position of samples, because sandstones having high $L_{sm} + Q_p$ ratios in the lower Galice Formation were found interbedded with those having low $L_{sm} + Q_p$ (Harper, 1980). Future work might determine whether these two detrital modes are correlated with different paleocurrent directions. The linear trends on the Q_p–L_v–L_{sm} and L_{sm}+Q_p–F–L_v diagrams (Fig. 7C and D) suggest mixing of two sources, one of which has a relatively constant F/L_v ratio (Fig. 7). The relatively constant F/L_v, the very common occurrence of plagioclase as phenocrysts in volcanic rock clasts, and the near absence of plutonic rocks in pebble conglomerates (Wyld, 1985; Seiders, 1991, written com-

mun., 1992) indicate that the plagioclase in the Galice sandstones is virtually all volcanic.

A sandstone that occurs within the upper pillow lavas of the Josephine ophiolite is too altered, including abundant patchy prehnite formed during ocean-ridge hydrothermal metamorphism (Harper, 1995), for accurate determination of a mode. Nevertheless, it is clearly similar to those within the lower turbidite of the Galice Formation, consisting of abundant volcanic (mostly microlitic) rock fragments, less common chert, and siliceous argillite clasts. The only major difference between this sandstone and that of the basal turbidite is a substantially lower plagioclase content than Galice sandstones, but this may be due to the replacement of plagioclase by prehnite.

Wyld (1985) and Seiders (1991, written commun., 1992) obtained detrital modes for conglomerates from the Galice Formation by point counting (Fig. 8). In their modal analysis, Wyld (1985) counted clasts larger than 1 mm, whereas Seiders (1991) counted clasts in the 0.5–6 cm diameter range. Galice conglomerates are rich in chert (C) and generally have very few quartzose sandstone clasts (Q; Fig. 8). The igneous component, which consists almost essentially of volcanic clasts, varies from near 0 to ~20%. This result implies a much lower proportion of volcanic clasts than in associated sandstones. Such a grain-size bias is evident in individual sandstone beds that have pebbly bases. Two of Wyld's (1985) conglomerate samples from the lower Galice Formation in the southern Klamath Mountains have much higher Q and are transitional between typical Galice Formation chert-rich conglomerates and correlative conglomerates of the Sierra Nevadan foothills (Fig. 8).

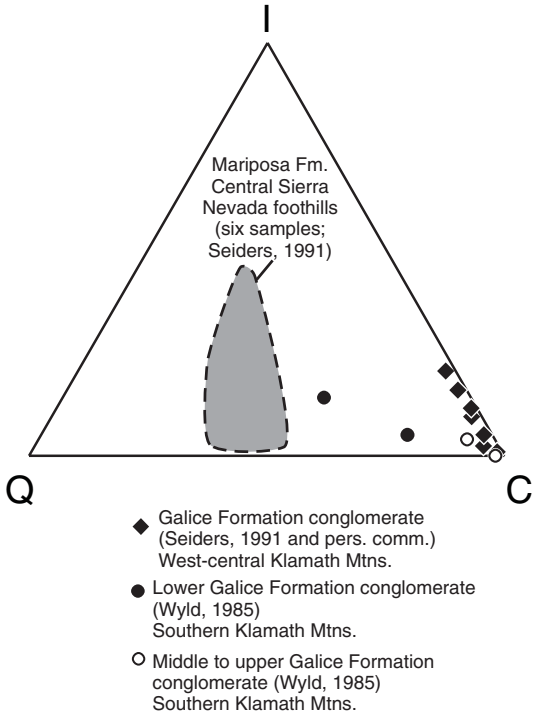

Figure 8. Conglomerate point count data for the Galice Formation and the Mariposa Formation in the central Sierran foothills illustrating provenance differences. I—igneous rocks; Q—quartz sandstone and quartzite; C—chert; Fm—formation. Data from Wyld (1985) and Seiders (1991, written commun., 1992).

HEAVY MINERALS

Occurrence

Snoke (1972, 1977), Harper (1980, 1984), and Wyld (1985) reported heavy-mineral assemblages in the Galice Formation. The most common heavy minerals are zircon (euhedral to very well rounded), tourmaline, apatite, biotite, muscovite, Cr-spinel, and, in volcanic-rich basal turbidite sandstones, clinopyroxene and hornblende. Less common to rare are garnet, epidote, staurolite, and glaucophane. The 2- to 5-cm-thick sandstone bed within the Josephine pillow lava unit has abundant clinopyroxene (~5 modal %), with lesser hornblende, Cr-spinel, and rare glaucophane (violet to clear pleochroism); zircon has not yet been found in this sample; these heavy minerals, as well as the detrital modes, are similar to those of volcanic-rich sandstones within the hemipelagic-turbidite transition zone and basal turbidite.

Cr-Spinel

McLennan et al. (1993) suggested that Cr-spinel most likely indicates an ophiolitic source area. Spinels can occur in any primitive mafic volcanic rocks, however, as well as in any type of ultramafic rock. Cookenboo et al. (1997) and Lee (1999) stressed the importance of using the chemical composition of detrital Cr-spinels to infer rock types in the source area. Lee (1999) suggested that Cr-spinels are significant in paleogeographic reconstructions because their deposition occurs within proximity of their source area.

Spinels from four sandstones were analyzed for this study. One sample is from the bed within the Josephine ophiolite pillow lava unit (sample PC-2b; Table 1), another sample from the basal Galice turbidite overlying the ophiolite (sample LJC-23; Table 1 and Fig. 2) and the other two samples from the turbidite sequence (samples DB-1 and CJ-7; Table 1 and Fig. 2). The Cr-spinels were analyzed with a JEOL 733 Superprobe at the Department of Earth and Environmental Sciences, Rensselaer Polytechnic Institute, Troy, New York, and with a JEOL 8900 electron microprobe at Binghamton University, Binghamton, New York. The elements Ti, Al, Cr, Mn, Mg, Ni, and Fe were analyzed using a 15-kV accelerating voltage, 15-nÅ beam current, and a 1-μm beam diameter. Elements Al, Cr, Mg, and Fe were counted for 40 seconds whereas Ti, Mn, and Ni were counted for 100 seconds each. Sample USNM 117075 from Tiebaghi Mine, New Caledonia, was used as an Al, Cr, Mg, and Fe standard at Rensselaer Polytechnic Institute. Other elemental standards used at Rensselaer Polytechnic Institute were rutile for Ti, tephroite for Mn, and diopside glass for Ni. Analy-

TABLE 1. REPRESENTATIVE ANALYSES OF Cr-RICH SPINEL

Sample	Locality*	TiO_2	Al_2O_3	Cr_2O_3	MnO	MgO	NiO	FeO	Fe_2O_3	Total	Cr^{3+}	Fe^{3+}	Al^{3+}	Mg#	Cr#
LJC-23†	Turbidite	0.63	21.09	39.66	0.35	9.67	0.15	18.01	10.35	99.91	0.48	0.13	0.38	0.44	0.56
LJC-23†	Turbidite	0.09	22.16	44.75	0.27	11.81	0.05	15.62	4.39	99.14	0.55	0.05	0.40	0.54	0.58
LJC-23†	Turbidite	b.d.#	33.28	31.93	0.21	13.77	0.10	14.03	5.26	98.64	0.37	0.06	0.57	0.60	0.39
LJC-23†	Turbidite	0.18	31.04	33.36	0.28	12.73	0.06	15.30	6.55	99.50	0.39	0.08	0.54	0.56	0.42
LJC-23†	Turbidite	b.d.#	16.11	50.77	0.40	9.15	0.08	18.69	4.48	99.76	0.64	0.05	0.30	0.44	0.68
LJC-23†	Turbidite	0.46	27.38	32.36	0.29	12.13	0.14	15.14	11.89	99.78	0.37	0.15	0.47	0.52	0.44
LJC-23†	Turbidite	0.21	12.80	51.33	0.30	9.99	0.06	16.31	9.01	100.01	0.64	0.12	0.24	0.47	0.73
LJC-23†	Turbidite	0.85	28.47	33.28	0.29	11.75	0.09	16.64	8.36	99.73	0.39	0.10	0.50	0.51	0.44
LJC-23†	Turbidite	b.d.#	31.39	35.26	0.21	14.06	0.15	13.53	3.84	98.49	0.41	0.04	0.55	0.62	0.43
LJC-23†	Turbidite	0.12	32.20	35.53	0.21	14.12	0.12	14.21	3.59	100.09	0.41	0.04	0.55	0.61	0.43
LJC-23†	Turbidite	0.21	16.26	45.95	0.39	8.96	0.05	17.99	9.71	99.52	0.57	0.13	0.30	0.42	0.65
LJC-23†	Turbidite	0.20	16.40	49.25	0.34	9.01	0.05	18.87	5.89	100.01	0.62	0.07	0.31	0.43	0.67
LJC-23†	Turbidite	b.d.#	13.87	47.99	0.38	9.33	0.09	16.81	11.30	99.82	0.59	0.15	0.26	0.44	0.70
LJC-23†	Turbidite	0.11	28.49	34.49	0.23	12.16	0.16	15.31	8.53	99.48	0.40	0.10	0.49	0.54	0.45
LJC-23†	Turbidite	0.14	19.36	46.28	0.29	11.44	0.13	15.27	6.22	99.13	0.57	0.08	0.35	0.53	0.62
LJC-23†	Turbidite	b.d.#	31.68	36.11	0.24	14.39	0.15	13.39	3.01	98.99	0.42	0.03	0.55	0.63	0.43
LJC-23†	Turbidite	1.40	19.93	37.83	0.26	12.01	0.24	14.69	12.80	99.16	0.46	0.18	0.36	0.52	0.56
LJC-23†	Turbidite	0.11	10.87	54.23	0.36	7.80	0.06	19.44	7.15	100.02	0.70	0.09	0.21	0.38	0.77
LJC-23†	Turbidite	1.31	19.86	38.52	0.22	11.83	0.14	15.13	12.59	99.61	0.47	0.17	0.36	0.52	0.57
CJ-7†	Turbidite	b.d.#	8.51	58.22	0.34	8.41	0.01	18.53	6.61	100.71	0.75	0.08	0.16	0.41	0.82
DB-1§	Turbidite	0.04	35.73	29.77	0.15	14.87	0.15	5.99	11.99	98.70	20.37	8.38	18.90	0.66	0.52
DB-1§	Turbidite	0.11	27.22	35.25	0.27	12.47	0.19	8.21	16.43	100.15	24.12	11.49	14.40	0.54	0.63
DB-1§	Turbidite	0.19	16.82	41.40	0.42	8.88	0.03	10.15	20.29	98.17	28.33	14.19	8.90	0.40	0.76
DB-1§	Turbidite	0.03	29.13	38.60	0.29	14.39	0.09	5.78	11.56	99.87	26.41	8.09	15.41	0.66	0.63
DB-1§	Turbidite	0.07	8.01	56.85	0.46	7.64	0.03	8.84	17.68	99.58	38.90	12.37	4.24	0.40	0.90
DB-1§	Turbidite	0.24	15.64	41.66	0.36	7.99	0.07	11.29	22.59	99.85	28.50	15.80	8.28	0.35	0.78
DB-1§	Turbidite	0.02	30.84	38.16	0.30	13.68	0.16	5.92	11.84	100.91	26.11	8.28	16.32	0.64	0.62
PC-2b§	Intra-pillow	0.14	12.96	43.93	0.53	5.53	0.10	11.04	22.09	96.32	30.06	15.45	6.86	0.28	0.81
PC-2b§	Intra-pillow	0.24	14.44	49.40	0.33	14.67	0.13	6.75	13.50	99.47	33.80	9.44	7.64	0.63	0.82
PC-2b†	Intra-pillow	b.d.#	29.97	36.50	0.26	12.42	0.09	15.92	4.29	99.45	0.43	0.05	0.52	0.55	0.45
PC-2b†	Intra-pillow	b.d.#	13.96	54.91	0.37	9.85	0.09	17.86	0.48	97.58	0.72	0.01	0.27	0.49	0.73
PC-2b†	Intra-pillow	0.25	14.89	50.36	0.37	9.20	0.04	18.16	6.37	99.64	0.64	0.08	0.28	0.44	0.69
PC-2b†	Intra-pillow	0.13	27.22	35.01	0.33	11.33	0.15	15.96	8.25	98.37	0.42	0.10	0.48	0.51	0.46
PC-2b†	Intra-pillow	b.d.#	29.25	37.70	0.28	12.25	0.09	16.28	3.79	99.67	0.44	0.04	0.51	0.55	0.46
PC-2b†	Intra-pillow	b.d.#	16.56	51.52	0.36	10.26	0.05	17.37	2.95	99.13	0.65	0.03	0.31	0.49	0.68
PC-2b†	Intra-pillow	1.31	17.76	23.55	0.30	7.66	0.22	20.10	29.57	100.48	0.27	0.42	0.30	0.32	0.47
PC-2b†	Intra-pillow	b.d.#	30.27	36.97	0.26	12.32	0.13	16.48	3.80	100.23	0.43	0.04	0.53	0.55	0.45
PC-2b†	Intra-pillow	b.d.#	28.07	39.18	0.16	12.61	0.06	15.71	3.22	99.10	0.47	0.04	0.50	0.57	0.48

Note: The ferric iron content of each analysis was determined by assuming stoichiometry, following the methods of Barnes and Roeder (2001).
*From Figure 2.
†Sample analyzed at Rensselaer Polytechnic Institute.
§Sample analyzed at Binghamton University.
#b.d.—below detection limits.

sis of the standard USNM 117075 was done throughout the session at Rensselaer Polytechnic Institute to assess proper calibration. Standards used at Binghamton University were TiO_2 for Ti, Al_2O_3 for Al, chromite for Cr, spessartine garnet for Mn, MgO for Mg, Ni-metal for Ni, and hematite for Fe.

The compositions of detrital spinels from the sandstone within the Josephine ophiolite pillow lava unit and the sandstone from the basal turbidite are given in Table 1 and are plotted in Figures 9 and 10. The detrital spinels show a wide range of compositions. Some plot entirely within the field for mantle peridotites, whereas others plot entirely in the field for volcanic spinels, including the mid-ocean ridge basalt (MORB) field and between the MORB and ocean-island—or within-plate—basalt (OIB) fields (Fig. 9). Other detrital spinels plot in the area of overlap for volcanic and mantle peridotite spinels (Fig. 9).

Those detrital spinels identified as originating from mantle peridotites in Figure 9 have Cr/(Cr + Al) ratios (Cr#) that overlap those of abyssal (mid-ocean ridge origin) and supra-subduction zone (SSZ) peridotites (Fig. 10A). All, however, have $Mg/(Mg + Fe^{2+})$ ratios that are lower than those for abyssal peridotite spinels; the $Mg/(Mg + Fe^{2+})$ ratios for all the detrital mantle spinels fall within the field for SSZ peridotites,

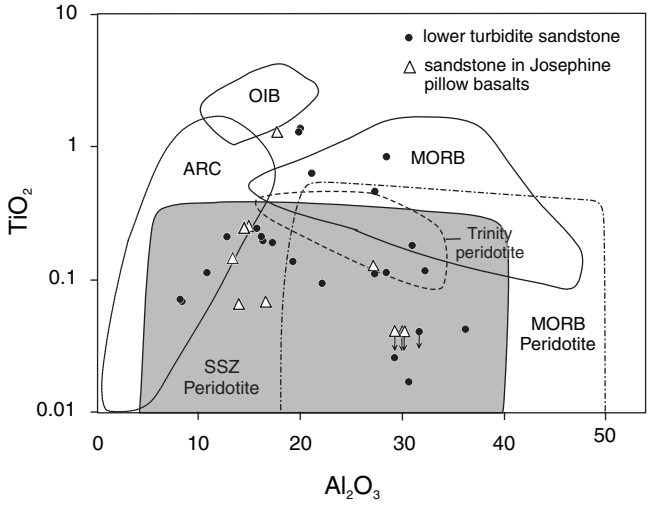

Figure 9. Al_2O_3 vs. TiO_2 diagram showing detrital Cr-spinels from an intra-pillow sandstone in the Josephine ophiolite and a turbidite sandstone of the Galice Formation. Fields are from Kamenetsky et al. (2001). This diagram is a good discriminator for tectonic setting as well as for distinguishing volcanic from peridotite spinels. OIB—ocean-island (within-plate) basalt; MORB—mid-ocean ridge basalt; SSZ—supra-subduction zone. Also shown is the field for spinels from the Trinity peridotite (Quick, 1981).

a result that implies that they are all derived from SSZ ophiolites (Fig. 10A).

Those detrital spinels identified as volcanic (MORB to MORB-OIB) in Figure 9 have Cr/(Cr + Al) ratios similar to the upper range of most modern MORB, but are shifted to lower Mg/(Mg + Fe^{2+}) ratios (Fig. 10B). This shift to lower Mg/(Mg + Fe^{2+}) ratios is probably due, in part, to the OIB component that is indicated in Figure 9, as OIB basalts have Mg/(Mg + Fe^{2+}) ratios that extend to much lower values. However, it may also be due to crystal fractionation of olivine, which causes the Mg/(Mg + Fe^{2+}) of spinel to increase (Dick and Bullen, 1984; Kamenetsky et al., 2001; Fig. 10B).

Figure 10C shows those detrital Cr-spinels that could have been derived from either mantle peridotite or volcanic rocks based on the classification shown in Figure 9. Most of these spinels, as well as some of the peridotite spinels (Fig. 10A), have high Cr/(Cr + Al) ratios, indicative of high degrees of partial melting, which is typical of arcs (Dick and Bullen, 1984). Four of the detrital spinels from the turbidite sample and one from the intra-pillow sample have Cr/(Cr + Al) ratios of ~0.8, which is characteristic of boninites (Fig. 10C) and mantle that has undergone very high degrees of melting or mantle that has interacted with a boninitic magma (e.g., Dick and Bullen, 1984; Harper, 2004).

AGE OF SOURCE AREAS

The age of detrital zircons within Galice sandstones was studied by Miller and Saleeby (1995) and Miller et al. (2003)

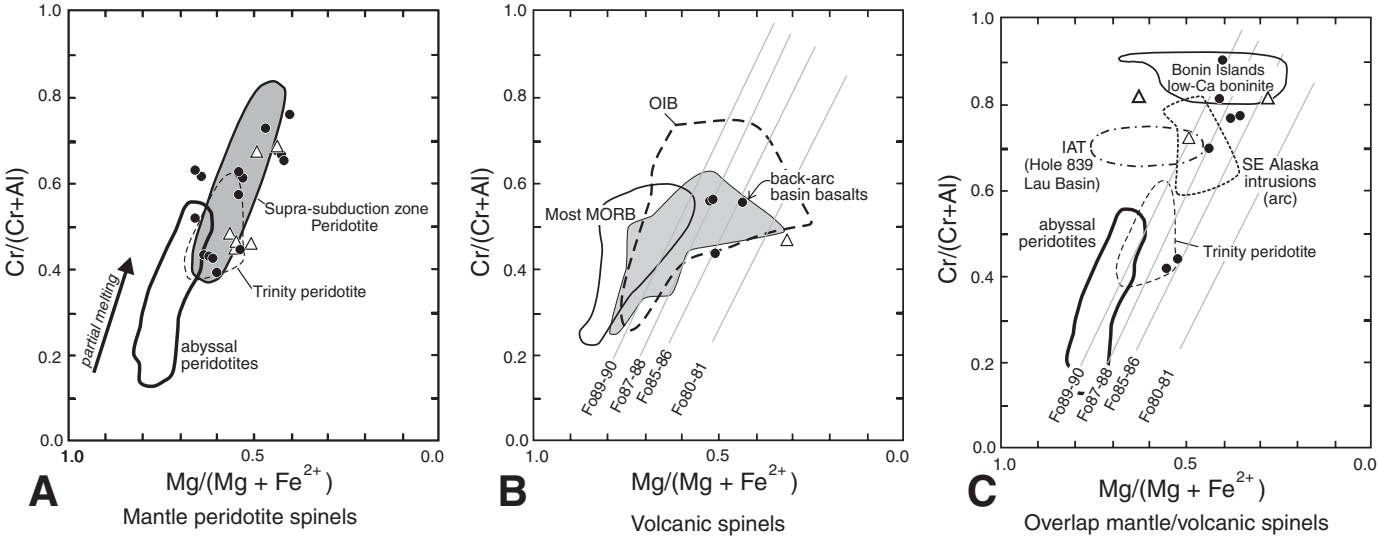

Figure 10. Cr/(Cr + Al) vs. Mg/(Mg + Fe^{2+}) diagram for detrital Cr-spinels from a sandstone within the pillow lavas of the Josephine ophiolite and a sandstone from the basal turbidite sequence overlying the ophiolite. Symbols are the same as in Figure 9. Field for Trinity peridotite from Quick (1981). Fields for MORB, southeastern Alaskan intrusions, and abyssal peridotites (MORB residue) from Dick and Bullen (1984); field for back-arc basin basalts from Dick and Bullen (1984), Hawkins and Melchoir (1985), Saunders and Tarney (1979; one sample); field for Hole 839 in the Lau Basin is from Allan (1994); field for low-Ca boninites is from Umino (1986); field for OIB from Kamenetsky et al. (2001); and field for supra-subduction zone peridotite is modified from Parkinson and Pearce (1998). Olivine isopleths are from Kamenetsky et al. (2001). A: Spinels derived from peridotite (as determined from Fig. 9). B: Spinels of volcanic origin (as determined from Fig. 9). C: Spinels that could be either volcanic or peridotitic origin (as determined from Fig. 9).

through U/Pb age dating. Miller and Saleeby (1995), using multiple grain fractions from various localities throughout the Galice Formation, obtained U-Pb data that plot as a chord on a concordia diagram, with an average upper intercept of ca. 1600 Ma and a lower intercept of ca. 215 Ma, although the youngest zircons approach ca. 170 Ma. Surprisingly, Miller and Saleeby (1995) found no difference in the age distributions of euhedral and well-rounded (recycled) zircon populations. All four of their Galice samples show the same spread on a concordia diagram, which implies no major variations in the age of detrital zircons in these samples. A fifth sample gives an older upper-intercept age; however, this sample is not from the Galice Formation but from the Lems Ridge olistostrome that underlies the Galice, which probably represents a fragment of older Klamath basement in the western Klamath terrane that is correlative with the lower Mesozoic Rattlesnake Creek terrane (Ohr, 1987).

Recently, Miller et al. (2003) reported ion-microprobe single-crystal U/Pb ages for detrital zircons from a Galice Formation sandstone near the base of the turbidite sequence at a *Buchia concentrica* locality. Most zircons from this sample are Late Jurassic, averaging ca. 153 Ma. Zircons of ca. 227 Ma are common, and a few Paleozoic and Proterozoic zircons were found. The high proportion of volcanic clasts in the sandstone, including altered glass, indicates erosion of an active arc; thus, the ca. 153-Ma age most likely approximates the time of turbidite deposition, consistent with the Late Jurassic age of the Galice turbidite.

The Nd and Sr isotopic values for slates from the Galice Formation turbidite sequence are rather uniform and indicate derivation from both Precambrian continental rocks and young mantle-derived rocks (Frost et al., this volume). These workers also found that the continental isotopic signal is greater in slates than in sandstones of the turbidite sequence, a relationship that may be consistent with differences in the whole-rock geochemistry discussed below.

Two chert pebbles from the Galice Formation were dated as Late Triassic using radiolaria (D.L. Jones, personal commun., 1979; Harper, 1980). One of the pebbles is from a volcanic-rich sandstone near the base of the turbidite sequence overlying the Josephine ophiolite, and the other pebble is from a conglomerate near the base of the type Galice Formation overlying the Rogue Formation.

GEOCHEMISTRY

Major- and trace-element geochemistry of sedimentary rocks can provide invaluable information about the original tectonic setting and the provenance of a sedimentary unit (Roser and Korsch, 1986; McLennan et al., 1993). Unlike petrographic methods for tectonic discrimination that are limited to using coarser grain sizes, chemical analyses of sedimentary rocks have no grain-size restrictions (Roser and Korsch, 1986). McLennan (1989) notes, however, that concentrations of heavy minerals in sandstones can affect rare-earth-element (REE) abundances and

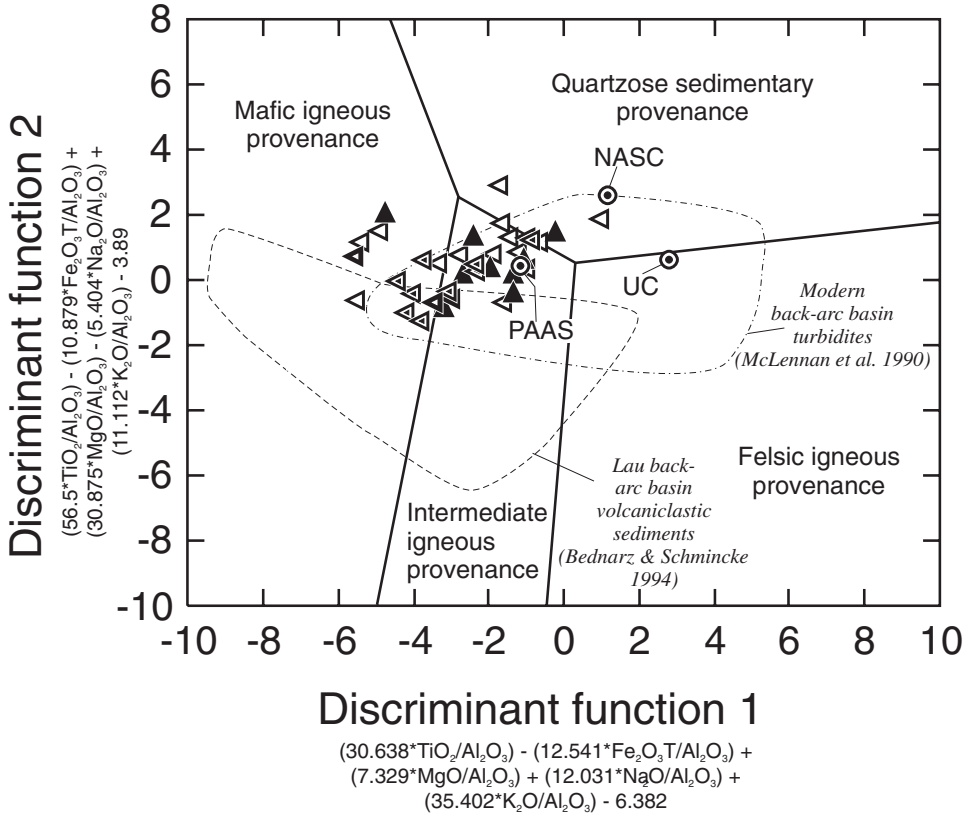

Figure 11. Provenance discriminant-function diagram of Roser and Korsch (1988). Only samples from the Galice turbidite are plotted. Siliceous argillite and chert from the hemipelagic sequence and Josephine ophiolite are not plotted because of their Fe-rich hemipelagic component. Also plotted are the average values for North American shale composite (NASC), post-Archean Australian shale composite (PAAS), upper continental crust (UC; Gromet et al., 1984; McLennan, 1989; McLennan, 2001), and fields for modern back-arc basin turbidites (McLennan et al., 1990) and volcaniclastic sediments from the Lau back arc (Bednarz and Schmincke, 1994). Symbols are the same as in Figure 5.

ratios, and that abundances of elements such as rare earths are diluted by the greater concentration of quartz in sandstones. Biogenic $CaCO_3$ or SiO_2 can also dilute concentrations of other elements within a sample (Roser and Korsch, 1986, 1988). Diagenetic reactions related to burial can affect silicate and calcite abundances of sandstones (Galloway, 1974). Thus, caution should be used when making interpretations based on geochemical analyses of sedimentary rocks, and ratios should be used when possible. Because we do not have CO_2 values for our analyses, we cannot correct for dilution resulting from $CaCO_3$. We have, thus, followed the advice of Roser and Korsch (1986, 1988) and recalculated major-element values on a CaO-free basis before plotting on some diagrams (e.g., Fig. 11).

Published and unpublished geochemical data for the Galice Formation are available from other studies (Coleman, 1972; Pinto-Auso and Harper, 1985; Kuhns and Baitis, 1987; Park-Jones, 1988; Zierenberg et al., 1988; Barnes et al., 1995; Frost et al., this volume; Table 2). In addition, we report a chemical analysis for a sandstone sample (D25C) that was analyzed along with samples of Park-Jones (1988) by X-ray fluorescence at McGill University. Only major-element data of Coleman (1972) are used, as his trace-element data are semiquantitative; sample

TABLE 2. SELECTED ANALYSES OF GALICE FORMATION SAMPLES

Sample*	22	24	30	33	65	89	102	139	147	37G	38G
Lithology	Slate	Slate	Slate	Slate	Slate	Slate	Slate	Slate	Slate	Graywacke	Graywacke
Locality	Type area	Type area	Type area	Type area	Type area	Type area	Type area	Type area	Type area	Type area	Type area
SiO_2	60.57	62.41	63.95	60.23	63.72	62.95	61.95	66.21	63.49	65.77	73.57
TiO_2	0.80	0.72	0.71	0.80	0.72	0.79	0.82	0.60	0.70	0.71	0.76
Al_2O_3	17.49	17.12	15.86	18.29	16.29	17.15	16.93	13.35	15.52	16.75	11.26
Fe_2O_3T†	8.24	7.27	6.60	7.91	7.53	6.99	7.33	7.37	7.49	5.80	6.32
MnO	0.16	0.06	0.07	0.07	0.03	0.08	0.02	0.09	0.04	0.02	0.02
MgO	2.49	2.70	3.03	2.60	2.41	2.82	2.87	2.71	3.29	1.92	2.13
CaO	0.76	0.70	0.64	0.14	0.29	0.33	0.33	1.66	0.54	0.02	0.02
Na_2O	2.18	2.00	2.21	0.84	1.59	1.78	2.24	1.26	1.99	1.08	0.37
K2O	2.23	2.32	2.80	2.49	2.01	2.56	2.47	1.84	1.85	2.06	1.29
P_2O_5	0.32	0.32	0.12	0.14	0.20	0.19	0.21	0.61	0.38	0.08	0.12
LOI	5.32	5.07	4.26	6.75	5.47	4.72	5.26	4.13	5.05	6.13	4.47
Total	100.56	100.69	100.25	100.26	100.26	100.36	100.43	99.83	100.34	100.34	100.33
Ba§	638	584	856	756	439	726	674	494	597	635	383
Rb	70	71	86	83	61	84	71	54	53	52	39
Sr	147	135	172	86	117	171	105	116	114	60	42
Pb	12	15	20	16	13	19	17	12	13	12	14
Y	147	27	24	34	27	36	28	30	25	29	12
Zr	159	152	145	178	143	173	176	131	144	144	174
Ni	54	60	47	85	50	23	75	48	39	50	81
Cr	112	101	110	104	100	125	148	85	120	198	281
V	190	180	197	196	200	180	200	174	213	142	156
Cs	4.38	5.07	n.d.	n.d.	n.d.	n.d.	n.d.	n.d.	2.34	n.d.	1.32
Sc	24	24	n.d.	n.d.	n.d.	n.d.	n.d.	n.d.	27.2	n.d.	20.28
Th	9.83	9.46	n.d.	n.d.	n.d.	n.d.	n.d.	n.d.	6.91	n.d.	6.59
Hf	4.69	4.41	n.d.	n.d.	n.d.	n.d.	n.d.	n.d.	4.68	n.d.	5.43
Ta	0.90	0.95	n.d.	n.d.	n.d.	n.d.	n.d.	n.d.	0.61	n.d.	0.67
La	31.02	29.08	n.d.	n.d.	n.d.	n.d.	n.d.	n.d.	25.48	n.d.	25.19
Ce	62.64	60.26	n.d.	n.d.	n.d.	n.d.	n.d.	n.d.	50.86	n.d.	45.36
Nd	33.60	31.85	n.d.	n.d.	n.d.	n.d.	n.d.	n.d.	24.67	n.d.	18.66
Sm	7.71	7.02	n.d.	n.d.	n.d.	n.d.	n.d.	n.d.	6.28	n.d.	4.16
Eu	1.53	1.42	n.d.	n.d.	n.d.	n.d.	n.d.	n.d.	1.68	n.d.	0.89
Tb	1.15	1.09	n.d.	n.d.	n.d.	n.d.	n.d.	n.d.	0.93	n.d.	0.47
Yb	4.32	3.76	n.d.	n.d.	n.d.	n.d.	n.d.	n.d.	3.39	n.d.	2.15
Lu	0.54	0.47	n.d.	n.d.	n.d.	n.d.	n.d.	n.d.	0.47	n.d.	0.28

Notes: JO—overlies Josephine ophiolite; LOI—loss on ignition; n.d.—no data.

*Data from Park-Jones (1988) except sample D25c, which is previously unpublished.

†Fe_2O_3T—total iron as Fe_2O_3.

§If all trace elements reported, analysis of Ba, Rb, Sr, Pb,Y, Zr, Ni, Cr, and V by X-ray fluorescence; others by instrumental neutron activation analysis.

B6C from Pinto-Auso and Harper (1985) was not used because of its extremely high CaO concentration.

A metalliferous component in sediments is best detected using the ratio Al/(Al + Fe + Mn), which is <0.35 for modern metalliferous sediments and >0.5 for nonmetalliferous pelagic clay (Bostrom and Peterson, 1969; Bostrom, 1973). This component can be derived either from hydrothermal springs or precipitation from seawater (as with manganese nodules). Negative, rather than positive, Ce anomalies on REE patterns for samples overlying and within the Josephine ophiolite indicate a hydrothermal origin. Figure 4, from Pinto-Auso and Harper (1985), shows that siliceous argillite and chert samples from the hemipelagic sequence and pillow lava unit of the Josephine ophiolite fall along a mixing line between modern terrigenous and low-temperature hydrothermal sediments. As discussed above, samples from within the pillow lava unit of the Josephine ophiolite and from the lower 8 m of the hemipelagic sequence are not metalliferous, although most have a metalliferous component (i.e., Al/[Al + Fe + Mn] <0.5); in fact, the least metalliferous hemipelagic sediments actually occur within the pillow lavas. This is somewhat surprising, because stratiform massive-sulfide deposits of hydrothermal origin are present in the

G1	G2	G3	G4	G5	G6	G7	G8	G9	G10	D25c
Slate	Slate	Slate	Slate	Slate	Slate	Slate	Slate	Slate	Slate	Graywacke
JO	JO	JO	JO	JO	JO	JO	JO	JO	JO	JO
62.21	61.20	63.24	62.22	66.01	62.12	61.58	68.76	67.42	61.06	64.12
0.77	0.77	0.84	0.94	0.76	0.77	0.87	0.62	0.59	0.87	0.63
17.17	15.90	18.52	19.23	15.29	16.06	17.49	14.05	14.16	18.55	15.31
5.02	8.01	5.11	5.86	7.99	7.99	6.49	6.17	6.95	5.75	5.62
0.02	0.04	0.01	0.04	0.06	0.04	0.03	0.03	0.05	0.02	0.05
1.91	2.70	2.07	2.86	2.81	2.79	2.68	2.38	2.21	2.00	2.17
0.33	0.61	0.30	0.01	0.16	1.03	0.36	0.20	0.42	0.06	5.34
1.30	1.61	0.72	n.d.	0.64	1.05	0.03	1.65	1.84	0.27	1.98
3.68	2.86	4.00	3.38	2.49	2.78	3.47	2.11	1.84	3.74	1.78
0.20	0.22	0.02	0.09	0.21	0.22	0.18	0.16	0.20	0.18	0.08
7.16	5.75	5.43	5.42	4.26	5.70	6.08	3.86	4.46	7.76	3.25
99.77	99.67	100.26	100.05	100.68	100.55	99.26	99.99	100.14	100.26	100.33
949	781	1232	1487	887	758	923	748	591	1227	612
125	88	139	124	77	92	112	68	57	123	n.d.
89	95	90	72	83	122	82	92	121	51	n.d.
n.d.	11	31	27	34	35	25	34	32	34	n.d.
26	26	29	18	26	28	22	14	18	40	n.d.
157	169	180	181	173	170	166	141	143	178	n.d.
67	60	57	60	81	77	63	40	66	53	65
99	110	129	172	124	112	122	111	110	152	164
177	159	210	252	157	170	206	154	106	220	162
12.24	8.42	n.d.	n.d.	n.d.	n.d.	n.d.	n.d.	n.d.	n.d.	n.d.
26.19	21.44	n.d.	n.d.	n.d.	n.d.	n.d.	n.d.	n.d.	n.d.	n.d.
13.29	10.41	n.d.	n.d.	n.d.	n.d.	n.d.	n.d.	n.d.	n.d.	n.d.
5.06	5.78	n.d.	n.d.	n.d.	n.d.	n.d.	n.d.	n.d.	n.d.	n.d.
1.16	0.87	n.d.	n.d.	n.d.	n.d.	n.d.	n.d.	n.d.	n.d.	n.d.
37.51	30.76	n.d.	n.d.	n.d.	n.d.	n.d.	n.d.	n.d.	n.d.	n.d.
70.23	63.52	n.d.	n.d.	n.d.	n.d.	n.d.	n.d.	n.d.	n.d.	n.d.
34.72	31.49	n.d.	n.d.	n.d.	n.d.	n.d.	n.d.	n.d.	n.d.	n.d.
7.41	7.01	n.d.	n.d.	n.d.	n.d.	n.d.	n.d.	n.d.	n.d.	n.d.
0.99	1.42	n.d.	n.d.	n.d.	n.d.	n.d.	n.d.	n.d.	n.d.	n.d.
0.99	1.05	n.d.	n.d.	n.d.	n.d.	n.d.	n.d.	n.d.	n.d.	n.d.
4.19	3.66	n.d.	n.d.	n.d.	n.d.	n.d.	n.d.	n.d.	n.d.	n.d.
0.55	0.49	n.d.	n.d.	n.d.	n.d.	n.d.	n.d.	n.d.	n.d.	n.d.

Josephine ophiolite (Kuhns and Baitis, 1987; Zierenberg et al., 1988), but are apparently the result of dilution by abundant terrigenous detritus, as indicated by Figure 4. "Off-axis" metalliferous sediments are present 8–23 m above the base of the hemipelagic sequence (Fig. 2), either due to precipitation from low-temperature, off-axis springs (Pinto-Auso and Harper, 1985) or from distal fallout of high-temperature springs at a younger, propagating spreading center (Harper, 2003). All slate and sandstone samples from the Galice turbidite, including those from the Elk outlier, have Al/(Al + Fe + Mn) ratios >0.5 (Fig. 4), indicating a negligible metalliferous component.

Interpretations about source area and tectonic setting based on sediment geochemistry can be made from several plots (Figs. 11, 12, and 13). The majority of the turbidite samples, including those from the Elk outlier, plot in the intermediate-igneous and mafic-igneous provenance fields on Figure 11 (Roser and Korsch, 1988), which uses linear equations of major-element ratios except for CaO and SiO_2 (because they can be elevated by biogenic contributions). The remaining turbidite samples plot in and near the quartzose sedimentary provenance field (Fig. 11). Samples from the hemipelagic sequence and pillow lava unit are not plotted on Figure 11 because their high-Fe hydrothermal components cause these samples to plot far to the left. Figure 11 also shows that Galice turbidite samples fall within the field for back-arc basin turbidites of McLennan et al. (1990) and are displaced away from average continental crust (UC) and sediments largely derived from continental crust (NASC and PAAS in Fig. 11).

Figure 12 uses the trace elements Th, Zr, and Sc, which are generally immobile during metamorphism. This diagram is useful in that sediments typical of passive continental margins have elevated Zr/Sc ratios due to zircon enrichment through sediment recycling (McLennan et al., 1993; Fig. 12). Active-margin samples, however, plot along a trend between mafic and continental sources. Figure 12 shows that the Galice Formation samples plot along this trend, indicating insignificant sediment recycling, although the presence of well-rounded detrital zircons in sandstones indicates some recycling has occurred (Harper, 1980; Miller and Saleeby, 1995). Figure 11 suggests that the Galice samples were derived, on average, from sources that are more mafic than typical continental crust; perhaps from the mixing of continental and intermediate arc material. The chert sample from the hemipelagic sequence above the Josephine pillow lavas plots at significantly higher Zr/Sc values compared to other samples (Fig. 12); although the nonbiogenic component in the chert should consist of terrigenous or tuffaceous material similar to that in the hemipelagic rocks and thus plot along the same trend as other Galice samples. Hence, it may not be valid to plot cherts on this diagram (McLennan et al., 1993). Moreover, the analytical uncertainties for Zr and Sc are relatively high for this particular sample since they are so diluted by SiO_2.

A more complete comparison of Galice samples with post-Archean Australian shale (PAAS), derived largely from continental sources, can be made by normalizing immobile trace and rare-earth elements to PAAS (Fig. 13). McLennan (1989) suggested that samples should be normalized to PAAS rather than to North American shale composite (NASC), due to the possible inclusion of abnormal samples in NASC. Reference samples are shown in Figure 13A and B for comparison with those from the Galice Formation. The NASC and average upper continental crust generally have flat PAAS-normalized patterns (Fig. 13A), reflecting the dominantly continental sources for the shale

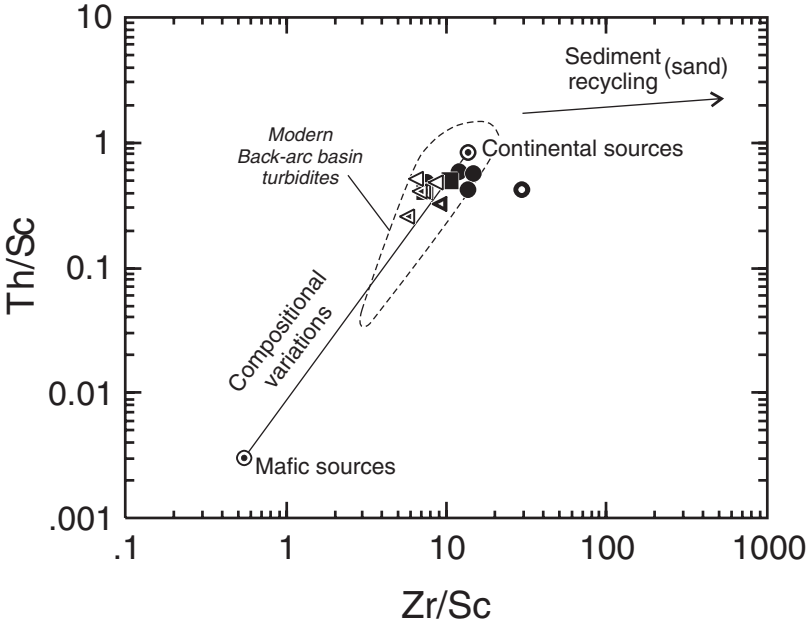

Figure 12. Th/Sc vs. Zr/Sc plot modified from McLennan et al. (1993) by the addition of average upper continental crust (representing cratonic sources; McLennan, 2001), a modern island-arc tholeiite (representing mafic sources; Pearce et al., 1995), and the field for modern back-arc basin turbidities (McLennan et al., 1990). Symbols are the same as in Figure 4.

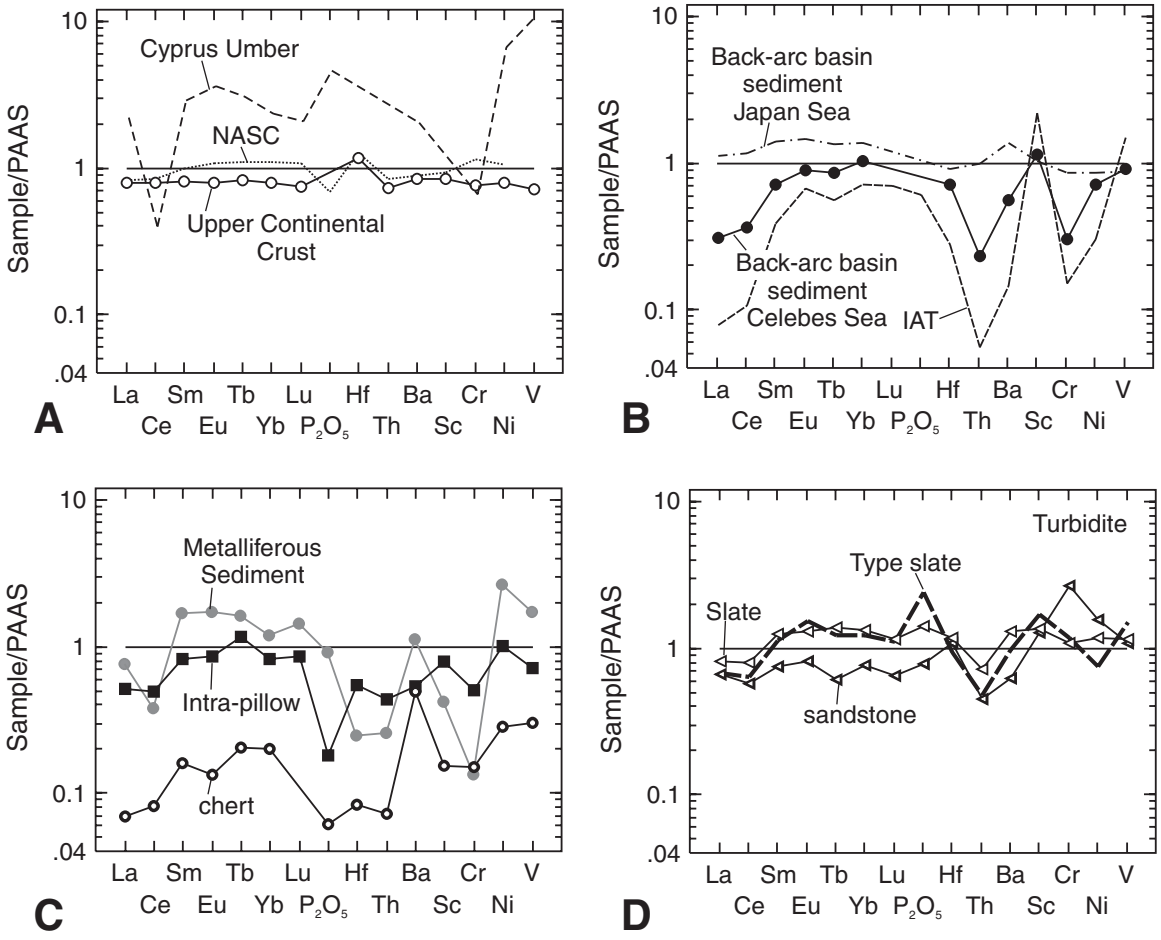

Figure 13. Post-Archean Australian shale composite (PAAS) normalized diagrams. (A) North American shale composite (NASC) from Gromet et al. (1984), Cyprus umber from Ravizza et al. (1999), and upper continental crust value from McLennan (2001). (B) Back-arc basin sediments (Japan and Celebes Seas) from McLennan et al. (1990) and modern island-arc tholeiite (IAT) from Pearce et al. (1995). (C) Chert from the hemipelagic sequence and typical metalliferous and intra-pillow argillites. (D) Typical slate and sandstone from the turbidite overlying the Josephine ophiolite, and a typical slate from the type area of the Galice Formation. Normalization values are from McLennan (1989).

composites. A Cyprus umber, which is essentially pure metalliferous sediment, shows enrichment with respect to PAAS, especially in Ni and V, except for negative Ce and Cr anomalies (Fig. 13A). The back-arc basin sediment from the Celebes Sea and an average island-arc tholeiite (IAT) have remarkably similar PAAS-normalized patterns (Fig. 13B); both are depleted in the light REEs compared to PAAS, have negative Hf, Th, and Cr anomalies, and have positive Sc anomalies (Fig. 13B). Back-arc basin sediment from the Japan Sea has a flatter PAAS-normalized pattern and a positive Ba anomaly (Fig. 13B), which is probably due to a large continental, or calc-alkaline volcanic, source component; this sample displays a slight negative slope from La through Eu, a result that is similar to the IAT sample and the Celebes Sea back-arc basin sediment (Fig. 13B).

Galice Formation slate from the type area and from the turbidite sequence overlying the Josephine ophiolite has similar patterns when normalized to PAAS (Fig. 13C). They show depletion in light REEs, a negative Th anomaly, and a positive P_2O_5 anomaly. A sandstone from the basal part of the turbidite overlying the Josephine ophiolite has a similar pattern to the slates, except for a negative Ba anomaly and positive Hf, Sc, and Cr anomalies (Fig. 13D). The Cr anomaly is probably from detrital Cr-spinel, as it is common in thin section, and the Sc anomaly is probably from the presence of detrital augite, which is abundant in this and most sandstone from the basal turbidite overlying the Josephine ophiolite (Harper, 1980).

The intra-pillow siliceous argillite, which is interbedded with pillow lavas of the Josephine ophiolite, has a similar pattern to slate from the Galice Formation turbidite (Fig. 13C), suggesting a similar terrigenous source. This sample, however, has

a negative rather than a positive P_2O_5 anomaly; however, because only one of the slates has a significant P_2O_5 anomaly and the sandstone has none, P may have been mobile during diagenesis and metamorphism. The pattern for the sandstone sample (Fig. 13D) is shifted downward relative to the slates, a relationship that is readily explained by dilution from biogenic silica, which is evident in thin section from the presence of radiolarians. As expected, this dilution effect is even greater for the chert from the hemipelagic sequence overlying the Josephine ophiolite (Fig. 13C). The pattern for the chert is similar to that for the intrapillow siliceous argillite (Fig. 13C), suggesting a similar terrigenous component, although the chert has a prominent positive Ba anomaly of unknown origin (seawater?), similar to the metalliferous sediment. The metalliferous sediment sample has a pattern that has similarities to both the slates of the Galice turbidite and to the Cyprus umber (e.g., negative Ce and Cr anomalies); this observation is consistent with the conclusion of Pinto-Auso and Harper (1985) that the metalliferous sediments in the hemipelagic sequence all have substantial terrigenous components, as evident from elevated Al/(Al + Fe + Mn) ratios (Fig. 4).

DISCUSSION

Provenance

Plots of detrital modes (Fig. 7), sediment geochemistry (Figs. 11, 12, and 13), and Nd and Sr isotopes (Frost et al., this volume) show trends for Galice turbidite samples that can be explained by mixing between two sources. The abundance of volcanic rock fragments in sandstones and conglomerates (Figs. 7 and 8) indicates that one of these sources is volcanic, and this source is almost certainly a magmatic arc. The non-arc source could represent basement of the arc, or a geographically distinct continental-like source.

The microlitic texture of most volcanic clasts suggest that the arc source was composed primarily of andesite, although the abundance of detrital clinopyroxene (up to 5 modal %) is perhaps more consistent with a basaltic-andesite or basalt source. A negative slope for light REE, negative Th anomaly, and positive Eu and Sc anomalies for Galice turbidite samples on a PAAS-normalized diagram (Fig. 13) are also suggestive of a mafic source. In addition, the trend in Figure 11 extends from the field for mafic, rather than intermediate, igneous provenances. The Nd and Sr isotope data for slates from the Galice Formation suggest that the arc was ensimatic (i.e., built on noncontinental basement). The high lithic content and generally low modal monocrystalline quartz in sandstones (Fig. 7B), along with the paucity of plutonic clasts in conglomerates (<3%, nearly all <1%; Wyld, 1985; Seiders, 1991, written commun., 1992) indicate that the arc was essentially undissected. Many of the sandstones plot in the transitional (partially dissected) arc field of the Q–F–L diagram (Fig. 7A), but this is a result of the inclusion of the chert clasts within Q. Nevertheless, several samples, especially those from the southern Klamath Mountains (Wyld, 1985), have sufficiently low total lithic clasts, relative to quartz and feldspar that they plot in the transitional arc field on a Q_m–F–L_t diagram (Fig. 7B). This may also be artificial, however, for the following reasons: Wyld's (1985) samples generally have >30% matrix, which is far higher than modern turbidites suggesting a post-depositional reduction of the L_t/F and L_t/Q_m ratios through the breakdown of lithic clasts; Wyld's (1985) reported "matrix" in her point-count tables includes both orthomatrix and pseudomatrix (i.e., Dickinson, 1970), and thus lithic clasts are underrepresented in the Q_m–F–L_t diagram; and Wyld's (1985) conglomerate samples have <3% plutonic clasts. Ingersoll (1978, 1983) suggested that pseudomatrix >20% should be a cautionary sign when analyzing point-count data.

Detrital modes of sandstone and conglomerate indicate that the non-arc component (source 2 on Fig. 7C and D) consisted almost entirely of chert and siliceous argillite. The inferred end member corresponding to this source component is essentially a lithic recycled component, in the terms of Figure 7B. The scarce metamorphic rock fragments (phyllite, quartz-mica tectonite, and quartzite) are attributed to this source, as are heavy minerals that are typically metamorphic in origin (garnet, glaucophane, epidote, and muscovite). The staurolite is originating from an unknown source area (Snoke, 1977; Harper, 1980). Ophiolitic rocks were also part of the non-arc source, as evident from detrital Cr-spinel compositions that indicate the presence of mantle peridotites, at least some of which were part of supra-subduction zone ophiolites (Figs. 9 and 10). Cr-spinels with compositions that indicate derivation from MORB and transitional MORB-OIB basalts (Fig. 9) were probably derived from non-SSZ ophiolites. A positive Cr anomaly on a PAAS-normalized diagram for a Galice sandstone (Fig. 13) is readily interpreted as due to the presence of detrital Cr-spinel. In contrast, an ophiolitic signature (high Cr or Ni) is not evident in the slates.

Extrapolation of the trend on Figure 11 suggests that the non-arc sources lie in the field of quartzose sedimentary province. The Th/Sc versus Zr/Sc diagram is compatible with this interpretation in that many of the samples plot close to continental sources (Fig. 12), but this diagram also shows that highly mature sands resulting from recycling, such as those formed along passive rifted margins, are not a significant component of Galice sandstones. Mature sandstones were present in the source area, however, based on the presence of very well rounded zircon in sandstone. Precambrian zircon is also present in the euhedral zircon population from Galice sandstones (Miller and Saleeby, 1995), indicating that at least some Precambrian sediment is first cycle. Overall, Miller et al. (2003) found that only a small fraction of the detrital zircons are Precambrian. Frost et al. (this volume) conclude from Nd and Sr isotope data that Galice slates have a significantly larger Precambrian continental component than do sandstones.

Snoke (1977) concluded that much of the detritus in Galice sandstones could be readily derived from older, more easterly terranes in the Klamath Mountains. This hypothesis is consistent with the west-directed flow indicated by paleocurrent data

from the Galice Formation where it overlies the Josephine ophiolite (Harper, 1980; Fig. 6D). The Klamath Mountains contain abundant chert and siliceous argillite, much of it Triassic (like two pebbles from the Galice Formation), as well as metamorphic and ophiolitic rocks (e.g., Irwin, 1966, 1972; Davis et al., 1978; Saleeby and Busby-Spera, 1992). The basement to all but the eastern Klamath arc rocks, including the Rogue–Chetco arc (Yule, 1996; Yule et al., this volume), is the early Mesozoic Rattlesnake Creek terrane (Wright and Wyld, 1994; Hacker et al., 1995). The Rattlesnake Creek terrane contains Triassic chert as well as mafic volcanic rocks that could have supplied MORB to MORB-OIB affinity detrital Cr-spinel (Fig. 9), although OIB affinity volcanic rocks are also present in the Sawyers Bar terrane of the central Klamath Mountains (Hacker et al., 1993). Units in the Klamath Mountains that could have supplied metamorphic detritus include the greenschist- to amphibolite-facies central metamorphic belt (e.g., Irwin, 1966; Davis et al., 1978). As for detrital glaucophane, the blueschist-facies Stuart Fork Terrane (Hotz et al., 1977) and Skookum Gulch Schist (Cotkin et al., 1992), as well as blueschist blocks in mélange of the Eastern Hayfork unit in the Sawyers Bar terrane (Wright, 1982; Hacker and Ernst, 1993), could have been the source(s). The large supra-subduction zone Trinity ophiolite could have supplied detrital peridotitic and boninitic Cr-spinel (Quick, 1981; Metcalf et al., 2000; Fig. 10).

Possible contributors of arc detritus from east of the Galice Formation include Middle Jurassic rocks in the eastern Klamath Mountains (e.g., Renne and Scott, 1988), the ca. 177- to 168-Ma Hayfork arc (western Hayfork terrane and related plutonic rocks; Wright and Fahan, 1988), and the ca. 159- to 165-Ma Wooley Creek plutonic belt (e.g., Hacker et al., 1995). These are not the appropriate age to have provided the ca. 153-Ma detrital zircons in the Galice Formation, nor are they likely to have yielded volcanic glass that is abundant in the volcanic-rich sandstones of the basal turbidite. Three plutons along the northeastern margin of the Klamath Mountains, however, may be the subvolcanic remains of a ca. 153-Ma zircon source. Irwin and Wooden (1999) reported 154- and 156-Ma U/Pb zircon ages for the Jacksonville and White Rock plutons in the northern Klamath Mountains, respectively, and Yule et al. (this volume) interpret an age of ca. 152–156 Ma from complex U/Pb zircon age data for the younger of two phases of the Ashland pluton. Frost et al. (this volume) suggest that the Rogue–Chetco arc (Fig. 1) was the source of the ca. 153-Ma volcanic detritus in Galice sandstones and slates, but this seems unlikely because: (1) the arc axis, probably represented by the plutonic Chetco complex lies west of the Galice Formation, inconsistent with paleocurrent data; (2) U/Pb zircon ages for the Chetco Complex are too old, ranging from 160 to 157 Ma (Yule, 1996; Yule et al., this volume); (3) the Rogue Formation underlies the Galice Formation and is thus too old, although one $^{40}Ar/^{39}Ar$ hornblende age is 153.4 Ma (Hacker et al., 1995); and (4) some of the components in the sandstones (e.g., glaucophane) are not known from the basement rocks of the Rogue–Chetco arc complex, which are dominantly ophiolitic (Yule, 1996; Yule et al., this volume). Volcanic members in the Galice Formation, which include coarse breccias, were obviously derived from nearby volcanic sources, but volcanic detritus in the Galice sandstones and slates had to have been mixed with non-arc sources before deposition.

Derivation of the ca. 227-Ma detrital zircons within the Galice Formation from the Klamath Mountain terranes to the east does appear unlikely, because there is no known source in the Klamath Mountains. The only known igneous rocks of the appropriate age in the Klamath Mountains are dacites in the Pit Formation of the eastern Klamath Mountains (Albers and Robertson, 1961), but these apparently are barren of zircon (J.E. Wright, written commun., 2004). Hacker et al. (1993) infer that arc rocks of this age are present in the Sawyers Bar terrane in the central Klamath Mountains, but even if they are, these rocks are predominantly mafic and unlikely to have yielded much zircon. The ca. 227-Ma detrital zircon, however, might be present in Upper Triassic to Middle Jurassic clastic rocks of the Klamath Mountains. A pre-Cretaceous reconstruction by Wyld and Wright (2001) places the Pine Nut terrane and the basinal Luning assemblage just east of the Klamath Mountains. Both the Pine Nut terrane and the Luning assemblage contain strata with peak detrital zircon ages of ca. 225 Ma (Manuszak et al., 2000), in addition to rocks of ca. 230 Ma in the former (Dilles and Wright, 1988); thus, these terranes are potential sources of the ca. 227-Ma detrital zircon in Galice sandstones.

South-directed paleocurrent directions in the type Galice Formation (Fig. 6B) suggest that the main source area for the Galice Formation may have been north of the present Klamath Mountains. Klamath rocks are covered by Cenozoic volcanic rocks to the north, but chert, including Triassic chert, (e.g., Pessagno and Whalen, 1982), and supra-subduction zone ophiolite peridotite (Bishop, 1995) are present in northeastern Oregon. Significant volumes of ca. 153-Ma volcanic rocks do not appear to be present (e.g., Saleeby and Busby-Spera, 1992), although some andesitic dikes and the Sunrise Butte pluton have K-Ar ages in the range of 150–158 Ma (Johnson et al., 1995). Only a few probable Late Jurassic arc rocks are exposed farther north in Washington (Miller et al., 1993). Possible source rocks for the ca. 227-Ma detrital zircons in the Galice may be present in the Blue Mountains, Oregon, Washington, and Idaho (e.g., 262- to 219-Ma Sparta complex and Carnian to Norian volcanic rocks of the Olds Ferry terrane; Avé Lallemant, 1995). The monocrystalline quartz-poor Galice sandstones are unlikely to have had a source to the south, because Paleozoic quartz sandstones in the central and southern Sierra Nevada contain zircons much older (>2.2 Ga) than detrital zircons in the Galice Formation (Harding et al., 2000).

Regional Variations

Miller et al. (2003) found that detrital-zircon age populations in a sandstone overlying the Ingalls ophiolitic complex in

the Cascade Mountains of Washington State were similar to ages from a sandstone of the Galice Formation, with peaks at ca. 153 and ca. 227 Ma. The Ingalls sandstone, however, contains no Precambrian zircon. No modal petrographic data are available for the Ingalls sandstones, although the types of clasts are similar to those in the Galice Formation, including Cr-spinel (Southwick, 1974; Miller et al., 1993).

Terranes similar to those of the western Klamath terrane are present in the Sierra Nevada region (Davis, 1969; Irwin, 2003). Conglomerates from the Mariposa Formation of the central Sierra Nevada foothills, which has long been correlated to the Galice Formation (e.g., Diller, 1907; Davis, 1969), are distinct from Galice conglomerates in that they have a much higher proportion of quartzose clasts (Seiders and Blome, 1988; Seiders, 1991, written commun., 1992; Fig. 8). This observation suggests a Sierran rather than Klamath Mountains source for the Mariposa Formation (Seiders and Blome, 1988), even though paleocurrent data reported by Bogen (1984) indicate south-southeast transport. Most of the conglomerates in the southernmost Galice Formation (Wyld, 1985; Fig. 1) are similar to those from the Galice Formation farther north, in which pebbles consist almost entirely of chert, argillite, or volcanic rocks, but some have elevated contents of quartzose clasts and are thus compositionally transitional to conglomerates of the Mariposa Formation (Fig. 8).

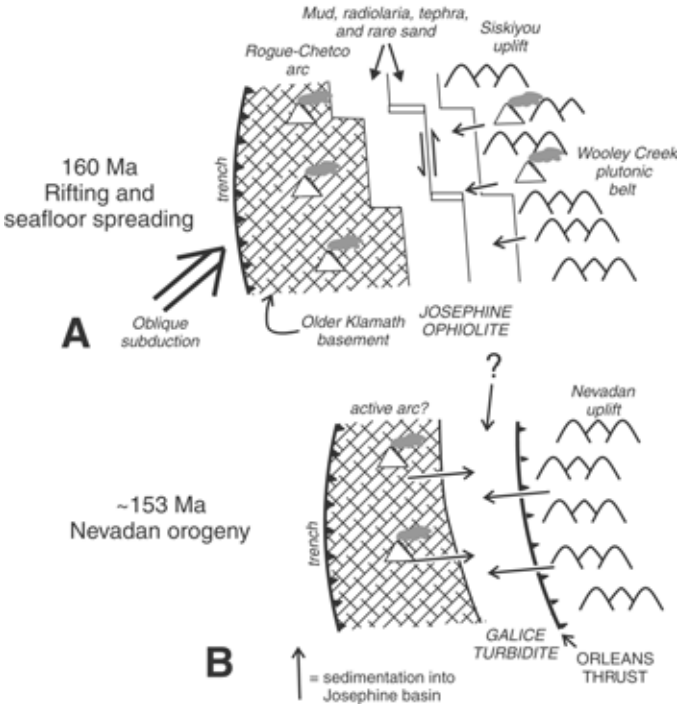

Figure 14. Tectonic model for the generation and emplacement of the Galice Formation and underlying Josephine ophiolite. The inferred oblique-subduction model is similar to the modern Andaman Sea. Arrows indicate probable paleocurrent flow directions. Modified from Harper and Wright (1984), Harper et al. (1985), Wyld and Wright (1988), and Harper et al. (1994). (A) Paleogeography prior to deposition of Galice turbidite. (B) Paleogeography during deposition of Galice turbidite.

Temporal Variations and Tectonic Implications

The ca. 162- to 153-Ma sedimentary rocks of the hemipelagic sequence, the hemipelagic-turbidite transition, and those within the Josephine ophiolite have similarities to the turbidite (Figs. 11, 12, and 13), except for the presence of a metalliferous (hydrothermal) component in some samples (Fig. 4). There is a striking similarity in petrography, and especially detrital Cr-spinel compositions (Figs. 9 and 10), between the thin sandstone bed within pillow lavas of the Josephine ophiolite (ca. 162 Ma) and sandstones of the lower Galice turbidite (ca. 153 Ma). This observation and similarities in the geochemistry of siliceous argillites and Galice slates suggest that the source area for the Galice turbidite was already established by ca. 162 Ma. This implies that the Galice source area was probably produced during ca. 165-Ma thrusting ("Siskiyou orogeny") that preceded formation of the Josephine ophiolite (Wright and Fahan, 1988; Hacker et al., 1995; Fig. 14). The inferred basin and source area relationships just after this episode of shortening are shown in Figure 14A.

Tectonic Setting of Deposition

The tectonic setting at ca. 160 Ma for the western Klamath Mountains is well constrained (e.g., Saleeby et al., 1982; Harper and Wright, 1984; Wyld and Wright, 1988; Hacker et al., 1995; Yule, 1996; Yule et al., this volume), and a model in which the Josephine ophiolite is located within a back-arc basin behind the west-facing Rogue–Chetco arc at ca. 160 Ma (Fig. 14A) is generally accepted (e.g., Dickinson et al., 1996). The ca. 177- to 168-Ma western Hayfork arc would represent a remnant arc at this time, and a tectonic highland is inferred because of a ca. 165-Ma shortening event (Wright and Fahan, 1988), sometimes called the "Siskiyou orogeny." Seafloor spreading in the back-arc basin is inferred to have been transform-dominated (Fig. 14A), based on the east-west orientation (in modern coordinates) of spreading centers inferred from sheeted dike orientations and other structural data (Harper et al., 1985; Alexander and Harper, 1992). Parts of both sides of this basin were underlain by older rifted Klamath crust, in places cut by Josephine-age mafic complexes; the Rogue–Chetco arc was built on older Klamath crust rifted away during seafloor spreading in the back-arc basin (Saleeby et al., 1982; Harper and Wright, 1984; Wyld and Wright, 1988; Yule, 1996; Yule et al., 1996).

Deposition of the Galice turbidite was interpreted by Harper and Wright (1984) and Wyld and Wright (1988) to have occurred in this basin before the Nevadan orogeny, with volcanic members derived from the Rogue–Chetco arc from the

west (Fig. 14A). This is probably the explanation for the high terrigenous content of sediments within the Josephine pillow lava unit and hemipelagic sequence, with the terrigenous sediment derived from the nearby "Siskiyou" highlands.

Based on the closeness in age of the Galice turbidite with the oldest plutons that cut the roof (Orleans) thrust, which may have >100-km displacement, Harper et al. (1994) reinterpreted the Galice turbidite as a synorogenic deposit (Fig. 14B). In this scenario, the turbidite was derived from Late Jurassic uplift related to underthrusting of the Josephine ophiolite. The area of uplift is inferred to have been similar to that affected by the pre-Josephine ("Siskiyou") deformation, which would account for the very similar clasts compositions and detrital modes of the sandstone within the Josephine pillow lavas (ca. 162 Ma) and the basal Galice turbidite (ca. 153 Ma). The great increase in amount of sandstone at the top of the hemipelagic-turbidite transition is based on the peak ca. 153-Ma age of detrital zircon in a sandstone from the basal turbidite (Miller et al., 2003) as well as other geochronologic constraints (Harper et al., 1994). Widespread ca. 150-Ma $^{40}Ar/^{39}Ar$ hornblende and mica cooling ages in the central Klamath Mountains (Hacker et al., 1995) may record Nevadan underthrusting and uplift.

The presence of the apparent hiatus at the top of the hemipelagic sequence (Pessagno and Blome, 1990; Pessagno et al., 2000), which is underlain by a zone of pre-cleavage deformation (Harper, this volume; Fig. 2), is enigmatic. As discussed above, this contact could be a minor unconformity, a normal fault, or a submarine landslide surface. A possible explanation for this surface is that it is a disconformity resulting from nonsedimentation and/or submarine erosion on a flexural bulge in front of the trench as the ophiolite and overlying Galice were thrust beneath older terranes of the Klamath Mountains during the Nevadan orogeny (Fig. 14). Passage of crust over a flexural bulge in front of a trench can result in an unconformity and normal faulting (e.g., Rowley and Kidd, 1981). Underthrusting of the Josephine ophiolite, which involved at least 40 km of displacement, is broadly analogous to subduction. In addition, relief created by this faulting could have resulted in a submarine landslide that removed strata prior to deposition of the hemipelagic-turbidite unit.

The quartzite-rich conglomerates in the Mariposa Formation in the Sierra Nevada foothills (Fig. 8) may indicate that the Mariposa and associated Late Jurassic arc rocks have not been translated appreciably relative to older rocks in the Sierra Nevada. If this suggestion is correct, then the Mariposa should contain >2.2-Ga detrital zircon known to be present in older rocks of the Sierra Nevada (Harding et al., 2000). Similarly, the Galice sandstones and conglomerates appear to be derived largely from the Klamath Mountains, except that there is no known Klamath source for ca. 227-Ma detrital zircons, and the location that provided ca. 153-Ma zircons is uncertain. Additional dating of zircon in the Klamath Mountains and elsewhere in the Cordillera might better constrain source areas for Galice sedimentary rocks and, in turn, better constrain models for Late Jurassic tectonics and paleogeography of western North America.

ACKNOWLEDGMENTS

Much of the data are from GDH's Ph.D. thesis at the University of California, Berkeley. Preparation of this manuscript was funded by National Science Foundation Grant EAR-0003444 to GDH. The Geology Department at San Jose State University kindly allowed JHM office space during preparation of this chapter. The Cr-spinel probe work was funded by the Department of Earth and Atmospheric Sciences, State University of New York (SUNY) Albany and a SUNY Albany Faculty Research Award Program grant to GDH. Reviews by Gary H. Girty and Raymond V. Ingersoll greatly improved this manuscript. Art Snoke proved to be a first-class editor. Helpful discussions were provided by Calvin G. Barnes, James E. Wright, and Bill Kidd. John Delano kindly allowed use of his lab for sample preparation, and Bill Blackburn was a great help to JHM on the microprobe.

APPENDIX

Figure A-1. Drill core sample from the Turner-Albright mine showing siliceous argillite that is interbedded with lavas of the Josephine ophiolite. The black and green laminations are interpreted as terrigenous and tuffaceous in origin, respectively. The alternating black and green colors are also typical of the hemipelagic sequence overlying the Josephine ophiolite. Note coin for scale.

REFERENCES CITED

Albers, J.P., and Robertson, J.F., 1961, Geology and ore deposits of East Shasta copper-zinc district, Shasta County, California: Washington, D.C., U.S. Geological Survey Professional Paper 338, 107 p.

Alexander, R., and Harper, G.D., 1992, The Josephine ophiolite, an ancient analog for oceanic lithosphere formed at slow/intermediate spreading centers, *in* Parson, B., et al., eds., Ophiolites and their modern oceanic analogues: London, Blackwell Scientific Publications, Geological Society Special Publication 60, p. 3–38.

Allan, J.F., 1994, Cr-spinel in depleted basalts from the Lau Basin backarc; Petrogenetic history from Mg-Fe crystal-liquid exchange, *in* Hawkins, J., et al., eds., Proceedings of the Ocean Drilling Program, Scientific results, volume 135: College Station, Texas, Ocean Drilling Program, p. 565–583.

Avé Lallemant, H.G., 1995, Pre-Cretaceous tectonic evolution of the Blue Mountains province, northeastern Oregon, *in* Vallier, T. L., and Brooks, H.C., eds., Geology of the Blue Mountains region of Oregon, Idaho, and Washington: Petrology and tectonic evolution of pre-Tertiary rocks of the Blue Mountains region: Reston, Virginia, U.S. Geological Survey Professional Paper 1438, p. 271–304.

Barnes, C.G., Donato, M.M., Barnes, M.A., Yule, J.D., Hacker, B.R., and Helper, M.A., 1995, Geochemical compositions of metavolcanic and metasedimentary rocks, western Jurassic and western Paleozoic and Triassic belts, Klamath Mountains, Oregon and California: Reston, Virginia, U.S. Geological Survey Open-File Report OF 95–0227-A, 63 p.

Barnes, S.J., and Roeder, P.L., 2001, The range of spinel compositions in terrestrial mafic and ultramafic rocks: Journal of Petrology, v. 42, p. 2279–2302, doi: 10.1093/petrology/42.12.2279.

Barrett, T.J., 1981, Chemistry and mineralogy of Jurassic bedded chert overlying ophiolites in the North Apennines, Italy: Chemical Geology, v. 34, p. 289–317, doi: 10.1016/0009-2541(81)90118-2.

Barrett, T.J., Taylor, P.N., and Lugowski, J., 1987, Metalliferous sediments from DSDP Leg 92; the East Pacific Rise transect: Geochimica et Cosmochimica Acta, v. 51, p. 2241–2253, doi: 10.1016/0016-7037(87)90278-X.

Bednarz, U., and Schmincke, H.-U., 1994, Composition and origin of volcaniclastic sediments in the Lau Basin (Southwest Pacific), Leg 135 (sites 834–839), *in* Hawkins, J., et al., eds., Proceedings of the Ocean Drilling Program, scientific results, volume 135: College Station, Texas, Ocean Drilling Program, p. 51–74.

Behrman, P.G., and Parkinson, G.A., 1978, Paleogeographic significance of the Callovian to Kimmeridgian strata, central Sierra Nevada Foothills, California, *in* Howell, D.G., and McDougall, K., eds., Mesozoic paleogeography of the western United States, Pacific Coast Paleogeography Symposium 2: Los Angeles, Pacific Section, Society of Economic Paleontologists and Mineralogists, p. 349–360.

Bishop, E.M., 1995, Mafic and ultramafic rocks of the Baker terrane, eastern Oregon, and their implications for terrane origin, *in* Vallier, T.L., and Brooks, H.C., eds., Geology of the Blue Mountains region of Oregon, Idaho, and Washington: Petrology and tectonic evolution of pre-Tertiary rocks of the Blue Mountains region: Reston, Virginia, U.S. Geological Survey Professional Paper 1438, p. 221–245.

Bogen, N.L., 1984, Stratigraphy and sedimentary petrology of the Upper Jurassic Mariposa Formation, western Sierra Nevada, California, *in* Crouch, J.K., and Bachman, S.B., eds., Tectonics and sedimentation along the California margin: Los Angeles, Pacific Section, Society of Economic Paleontologists and Mineralogists Field Trip Guidebook 38, p. 119–134.

Bogen, N.L., 1986, Paleomagnetism of the Upper Jurassic Galice Formation, southwestern Oregon; Evidence for differential rotation of the eastern and western Klamath Mountains: Geology, v. 14, p. 335–338, doi: 10.1130/0091-7613(1986)14<335:POTUJG>2.0.CO;2.

Bogen, N.L., Kent, D.V., and Schweickert, R.A., 1985, Paleomagnetism of Jurassic rocks in the western Sierra Nevada metamorphic belt and its bearing on the structural evolution of the Sierra Nevada Block: Journal of Geophysical Research, v. 90, p. 4627–4638.

Bostrom, K., 1973, The origin and fate of ferromanganoan active ridge sediments: Stockholm Contributions in Geology, v. 27, p. 149–243.

Bostrom, K., and Peterson, M.N.A., 1969, The origin of aluminum-poor ferromanganoan sediments in areas of high heat flow on the East Pacific Rise: Marine Geology, v. 7, p. 427–447, doi: 10.1016/0025-3227(69)90016-4.

Burchfiel, B.C., and Davis, G.A., 1981, Triassic and Jurassic tectonic evolution of the Klamath Mountains–Sierra Nevada geologic terrane, *in* Ernst, W.G, ed., The geotectonic development of California—Rubey Volume 1: Englewood Cliffs, New Jersey, Prentice-Hall, p. 50–70.

Cashman, S.M., 1988, Finite-strain patterns of Nevadan deformation, western Klamath Mountains, California: Geology, v. 16, p. 839–843, doi: 10.1130/0091-7613(1988)016<0839:FSPOND>2.3.CO;2.

Cater, F.W., Jr., and Wells, F.G., 1953, Geology and mineral resources of the Gasquet Quadrangle, California-Oregon: Washington, D.C., U.S. Geological Survey Bulletin 995-C, p. 79–133.

Coleman, R.G., 1972, The Colebrooke Schist of southwestern Oregon and its relation to the tectonic evolution of the region: Washington, D.C., U.S. Geological Survey Bulletin 1339, 61 p.

Cookenboo, H.O., Bustin, R.M., and Wilks, K.R., 1997, Detrital chromian spinel compositions used to reconstruct the tectonic setting of provenance; implications for orogeny in the Canadian Cordillera: Journal of Sedimentary Research, v. 67, p. 116–123.

Cotkin, S.J., Cotkin, M.L., and Armstrong, R.L., 1992, Early Paleozoic blueschist from the schist of Skookum Gulch, eastern Klamath Mountains, Northern California: Journal of Geology, v. 100, p. 323–338.

Davis, G.A., 1969, Tectonic correlations, Klamath mountains and western Sierra Nevada, California: Geological Society of America Bulletin, v. 80, p. 1095–1108.

Davis, G.A., Monger, J.W.H., and Burchfiel, B.C., 1978, Mesozoic construction of the Cordilleran "collage," central British Columbia to central California, *in* Howell, D.G., and McDougall, K., eds., Mesozoic paleogeography of the western United States, Pacific Coast Paleogeography Symposium 2: Los Angeles, Pacific Section, Society of Economic Paleontologists and Mineralogists, p. 1–32.

Dick, H.J.B., 1976, The origin and emplacement of the Josephine Peridotite of southwestern Oregon [Ph.D. dissertation]: New Haven, Connecticut, Yale University, 409 p.

Dick, H.J.B., and Bullen, T., 1984, Chromian spinel as a petrogenetic indicator in abyssal and alpine-type peridotites and spatially associated lavas: Contributions to Mineralogy and Petrology, v. 86, p. 54–76, doi: 10.1007/BF00373711.

Dickinson, W.R., 1970, Interpreting detrital modes of graywacke and arkose: Journal of Sedimentary Petrology, v. 40, p. 695–707.

Dickinson, W.R., 1985, Interpreting provenance relations from detrital modes of sandstones, *in* Zuffa, G.G., ed., Provenance of arenites, NATO ASI Series C: Mathematical and Physical Sciences v. 148, p. 333–361.

Dickinson, W.R., Beard, L.S., Brakenridge, G.R., Erjavec, J.L., Ferguson, R.C., Inman, K.F., Knepp, R.A., Lindberg, F.A., and Ryberg, P.T., 1983, Provenance of North American Phanerozoic sandstones in relation to tectonic setting: Geological Society of America Bulletin, v. 94, p. 222–235.

Dickinson, W.R., Hopson, C.A., Saleeby, J.B., Schweickert, R.A., Ingersoll, R.V., Pessagno, E.A., Jr., Mattinson, J.M., Luyendyk, B.P., Beebe, W., Hull, D.M., Munoz, I.M., and Blome, C.D., 1996, Alternate origins of the Coast Range Ophiolite (California); Introduction and implications: GSA Today, v. 6, p. 1–10.

Diller, J.S., 1907, The Mesozoic sediments of southwestern Oregon: American Journal of Science, v. 23, p. 401–421.

Dilles, J.H., and Wright, J.E., 1988, The chronology of early Mesozoic arc magmatism in the Yerington District of western Nevada and its regional implications: Geological Society of America Bulletin, v. 100, p. 644–652, doi: 10.1130/0016-7606(1988)100<0644:TCOEMA>2.3.CO;2.

Frei, L.S., 1986, Additional paleomagnetic results from the Sierra Nevada; Further constraints on Basin and Range extension and northward displacement in the western United States: Geological Society of America

Bulletin, v. 97, p. 840–849, doi: 10.1130/0016-7606(1986)97<840:APRFTS>2.0.CO;2.

Frost, C.D., Barnes, C.G., and Snoke, A.W., 2006, this volume, Nd and Sr isotopic data from argillaceous rocks of the Galice Formation and Rattlesnake Creek terrane, Klamath Mountains: Evidence for the input of Precambrian sources, *in* Snoke, A.W., and Barnes, C.G., eds., Geological studies in the Klamath Mountains province, California and Oregon: A volume in honor of William P. Irwin: Boulder, Colorado, Geological Society of America Special Paper 410, doi: 10.1130/2006.2410(05).

Galloway, W.E., 1974, Deposition and diagenetic alteration of sandstone in northeast Pacific arc-related basins; implications for graywacke genesis: Geological Society of America Bulletin, v. 85, p. 379–390, doi: 10.1130/0016-7606(1974)85<379:DADAOS>2.0.CO;2.

Garcia, M.O., 1982, Petrology of the Rogue River island-arc complex, southwest Oregon: American Journal of Science, v. 282, p. 783–807.

Giaramita, M.J., and Harper, G.D., 2006, this volume, Geochemistry of ophiolitic rocks associated with the western part of the Elk outlier of the western Klamath terrane, southwestern Oregon, *in* Snoke, A.W., and Barnes, C.G., eds., Geological studies in the Klamath Mountains province, California and Oregon: A volume in honor of William P. Irwin: Boulder, Colorado, Geological Society of America Special Paper 410, doi: 10.1130/2006.2410(08).

Gray, G.G., 1985, Structural, geochronologic, and depositional history of the western Klamath Mountains, California and Oregon; Implications for the early to middle Mesozoic tectonic evolution of the western North American Cordillera [Ph.D. dissertation]: Austin, University of Texas, 224 p.

Gray, G.G., 2006, this volume, Structural and tectonic evolution of the western Jurassic belt along the Klamath River corridor, Klamath Mountains, California, *in* Snoke, A.W., and Barnes, C.G., eds., Geological studies in the Klamath Mountains province, California and Oregon: A volume in honor of William P. Irwin: Boulder, Colorado, Geological Society of America Special Paper 410, doi: 10.1130/2006.2410(07).

Gromet, L.P., Dymek, R.F., Haskin, L.A., and Korotev, R.L., 1984, The "North American shale composite"; Its compilation, major and trace element characteristics: Geochimica et Cosmochimica Acta, v. 48, p. 2469–2482, doi: 10.1016/0016-7037(84)90298-9.

Hacker, B.R., and Ernst, W.G., 1993, Jurassic orogeny in the Klamath Mountains: A geochronological analysis, *in* Dunn, G., and McDougall, K., eds., Mesozoic paleogeography of the western United States—II: Los Angeles, Pacific Section, Society of Economic Paleontologists and Mineralogists, p. 37–59.

Hacker, B.R., Ernst, W.G., and McWilliams, M.O., 1993, Genesis and evolution of a Permian-Jurassic magmatic arc/accretionary wedge, and reevaluation of terranes in the central Klamath Mountains: Tectonics, v. 12, p. 387–409.

Hacker, B.R., Donato, M.M., Barnes, C.G., McWilliams, M.O., and Ernst, W.G., 1995, Timescales of orogeny: Jurassic construction of the Klamath Mountains: Tectonics, v. 14, p. 677–703, doi: 10.1029/94TC02454.

Harding, J.P., Gehrels, G.E., Harwood, D.S., and Girty, G.H., 2000, Detrital zircon geochronology of the Shoo Fly Complex, northern Sierra Terrane, northeastern California, *in* Soreghan, M.J., and Gehrels, G.E., eds., Paleozoic and Triassic paleogeography and tectonics of western Nevada and northern California: Boulder, Colorado, Geological Society of America Special Paper 347, p. 43–55.

Harper, G.D., 1980, Structure and petrology of the Josephine ophiolite and overlying metasedimentary rocks, northwestern California [Ph.D. dissertation]: Berkeley, University of California, 260 p.

Harper, G.D., 1984, The Josephine ophiolite, northwestern California: Geological Society of America Bulletin, v. 95, p. 1,009–1,026.

Harper, G.D., 1994, A review of hemipelagic and turbidite sedimentation associated with the Josephine Ophiolite, California: Ofioliti, v. 19, p. 397–411.

Harper, G.D., 1995, Pumpellyosite and prehnitite associated with epidosite in the Josephine ophiolite—Ca metasomatism during upwelling of hydrothermal fluids at a spreading axis, *in* Schiffman, P., and Day, H., eds., Low-grade metamorphism of mafic rocks: Boulder, Colorado, Geological Society of America Special Paper 296, p. 101–122.

Harper, G.D., 2003, Fe-Ti basalts and propagating rift tectonics in the Josephine Ophiolite: Geological Society of America Bulletin, v. 115, p. 771–787, doi: 10.1130/0016-7606(2003)115<0771:FBAPTI>2.0.CO;2.

Harper, G.D., 2004, Tectonic implications of boninite, arc tholeiite, and MORB magma types in the Josephine Ophiolite, California-Oregon, *in* Dilek, Y. and Robinson, P.T., eds., Ophiolites in Earth history: London, Blackwell Scientific Publications, Geological Society Special Publication 218, p. 207–229.

Harper, G.D., 2006, this volume, Structure of syn-Nevadan dikes and their relationship to deformation of the Galice Formation, western Klamath terrane, northwestern California, *in* Snoke, A.W., and Barnes, C.G., eds., Geological studies in the Klamath Mountains province, California and Oregon: A volume in honor of William P. Irwin: Boulder, Colorado, Geological Society of America Special Paper 410, doi: 10.1130/2006.2410(06).

Harper, G.D., and Park, R., 1986, Paleomagnetism of the Upper Jurassic Galice Formation, southwestern Oregon; Evidence for differential rotation of the eastern and western Klamath Mountains: Comment: Geology, v. 14, p. 1049–1050, doi: 10.1130/0091-7613(1986)14<1049:CAROPO>2.0.CO;2.

Harper, G.D., and Wright, J.E., 1984, Middle to Late Jurassic tectonic evolution of the Klamath Mountains, California-Oregon: Tectonics, v. 3, p. 759–772.

Harper, G.D., Saleeby, J.B., and Norman, E.A.S., 1985, Geometry and tectonic setting of sea-floor spreading for the Josephine ophiolite, and implications for Jurassic accretionary events along the California margin, *in* Howell, D.G., ed., Tectonostratigraphic terranes of the Circum-Pacific region: Houston, Circum-Pacific Council for Energy and Mineral Resources, Earth Science Series 1, p. 239–257.

Harper, G.D., Bowman, J.R., and Kuhns, R., 1988, Field, chemical, and isotopic aspects of submarine hydrothermal metamorphism of the Josephine ophiolite, Klamath Mountains, California-Oregon: Journal of Geophysical Research, v. 93, p. 4,625–4,657.

Harper, G.D., Saleeby, J.B., and Heizler, M., 1994, Formation and emplacement of the Josephine ophiolite and the age of the Nevadan Orogeny in the Klamath Mountains, California-Oregon: U/Pb zircon and $^{40}Ar/^{39}Ar$ geochronology: Journal of Geophysical Research, v. 99, p. 4293–4321, doi: 10.1029/93JB02061.

Harper, G.D., Giaramita, M.J., and Kosanke, S.B., 2002, Josephine and Coast Range Ophiolites, Oregon and California, *in* Moore, G.W., ed., Field guide to the geologic processes in Cascadia: Portland, Oregon, 98th Annual Meeting of the Cordilleran Section of the Geological Society of America Guidebook, p. 1–22.

Hawkins, J.W., and Melchior, J.T., 1985, Petrology of Mariana Trough and Lau Basin basalts: Journal of Geophysical Research, v. 90, p. 11,431–11,468.

Hotz, P.E., Lanphere, M.A., and Swanson, D.A., 1977, Triassic blueschist from northern California and north-central Oregon: Geology, v. 5, p. 659–663, doi: 10.1130/0091-7613(1977)5<659:TBFNCA>2.0.CO;2.

Imlay, R.W., Dole, H.M., Peck, D.L., and Wells, F.G., 1959, Relations of certain Upper Jurassic and Lower Cretaceous formations in southwestern Oregon: American Association of Petroleum Geologists Bulletin, v. 43, p. 2770–2785.

Ingersoll, R.V., 1978, Petrofacies and petrologic evolution of the Late Cretaceous fore-arc basin, northern and central California: Journal of Geology, v. 86, p. 335–352.

Ingersoll, R.V., 1983, Petrofacies and provenance of late Mesozoic forearc basin, northern and central California: American Association of Petroleum Geologists Bulletin, v. 67, p. 1125–1142.

Ingersoll, R.V., and Suczek, C.A., 1979, Petrology and provenance of Neogene sand from Nicobar and Bengal fans, DSDP sites 211 and 218: Journal of Sedimentary Petrology, v. 49, p. 1217–1228.

Ingersoll, R.V., Fullard, T.F., Ford, R.L., Grimm, J.P., Pickle, J.D., and Sares, S.W., 1984, The effect of grain size on detrital modes; A test of the Gazzi-Dickinson point-counting method: Journal of Sedimentary Petrology, v. 54, p. 103–116.

Irwin, W.P., 1960, Geologic reconnaissance of the northern Coast Ranges and Klamath Mountains, California, with a summary of the mineral resources: San Francisco, California Division of Mines and Geology Bulletin 179, 80 p.

Irwin, W.P., 1964, Late Mesozoic orogenies in the ultramafic belts of northwestern California and southwestern Oregon: Washington, D.C., U.S. Geological Survey Professional Paper 501-C, p. C1–C9.

Irwin, W.P., 1966, Geology of the Klamath Mountains province, *in* Bailey, E.H., ed., Geology of northern California: San Francisco, California Division of Mines and Geology Bulletin 190, p. 19–38.

Irwin, W.P., 1972, Terranes of the Western Paleozoic and Triassic belt in the southern Klamath Mountains, California: Washington, D.C., U.S. Geological Survey Professional Paper 800-C, p. C103–C111.

Irwin, W.P., 1994, Geologic map of the Klamath Mountains, California and Oregon: Reston, Virginia, U.S. Geological Survey Miscellaneous Field Investigations, I-2148, scale 1:500,000, 1 sheet.

Irwin, W.P., 2003, Correlation of the Klamath Mountains and Sierra Nevada: Reston, Virginia, U.S. Geological Survey Open-File Report 02–0490, 2 sheets.

Irwin, W.P., and Wooden, J.L., 1999, Plutons and accretionary episodes of the Klamath Mountains, California and Oregon: Reston, Virginia, U.S. Geological Survey Open-File Report 99–0374, 1 sheet.

Jachens, R.C., Barnes, C.G., and Donato, M.M., 1986, Subsurface configuration of the Orleans Fault; Implications for deformation in the western Klamath Mountains, California: Geological Society of America Bulletin, v. 97, p. 388–395, doi: 10.1130/0016-7606(1986)97<388:SCOTOF>2.0.CO;2.

Johnson, K., Walton, C., Barnes, C.G., and Kistler, R.W., 1995, Time-dependent geochemical variations of Jurassic and Cretaceous plutons in the Blue Mountains, northeastern Oregon: Geological Society of America Abstracts with Programs, v. 27, p. 435.

Jones, R.F., 1988, Structural geology of the northern Galice Formation, western Klamath Mountains, Oregon and California [M.S. thesis]: Albany, State University of New York, 211 p.

Kamenetsky, V.S., Crawford, A.J., and Meffre, S., 2001, Factors controlling chemistry of magmatic spinel; An empirical study of associated olivine, Cr-spinel and melt inclusions from primitive rocks: Journal of Petrology, v. 42, p. 655–671, doi: 10.1093/petrology/42.4.655.

Kays, M.A., 1968, Zones of alpine tectonism and metamorphism, Klamath Mountains, southwestern Oregon: Journal of Geology, v. 76, p. 17–36.

Kuhns, R.J., and Baitis, H.W., 1987, Preliminary study of the Turner Albright Zn-Cu-Ag-Au-Co massive sulfide deposit, Josephine County, Oregon: Economic Geology and the Bulletin of the Society of Economic Geologists, v. 82, p. 1362–1376.

Lee, Y.I., 1999, Geotectonic significance of detrital chromian spinel; A review: Geoscience Journal, v. 3, p. 23–29.

MacDonald, J.H., Jr., Harper, G.D., Miller, J.S., and Zhu, B., 2004, Petrology, provenance, and further age control of the Galice Formation, Klamath Mountains, Oregon-California: Geological Society of America Abstracts with Programs, v. 36, p. 36–37.

Mankinen, E.A., and Irwin, W.P., 1982, Paleomagnetic study of some Cretaceous and Tertiary sedimentary rocks of the Klamath Mountains province, California: Geology, v. 10, p. 82–87, doi: 10.1130/0091-7613(1982)10<82:PSOSCA>2.0.CO;2.

Manuszak, J.D., Satterfield, J.I., and Gehrels, G.E., 2000, Detrital zircon geochronology of Upper Triassic strata in western Nevada, *in* Soreghan, M.J., and Gehrels, G.E., eds., Paleozoic and Triassic paleogeography and tectonics of western Nevada and northern California: Boulder, Colorado, Geological Society of America Special Paper 347, p. 109–118.

McLennan, S.M., 1989, Rare earth elements in sedimentary rocks; Influence of provenance and sedimentary processes: Reviews in Mineralogy, v. 21, p. 169–200.

McLennan, S.M., 2001, Relationships between the trace element composition of sedimentary rocks and upper continental crust: Geochemistry, Geophysics, Geosystems—G^3, v. 2, doi: 2000GC000109.

McLennan, S.M., Taylor, S.R., McCulloch, M.T., and Maynard, J.B., 1990, Geochemical and Nd-Sr isotopic composition of deep-sea turbidites; Crustal evolution and plate tectonic associations: Geochimica et Cosmochimica Acta, v. 54, p. 2015–2050, doi: 10.1016/0016-7037(90)90269-Q.

McLennan, S.M., Hemming, S., McDaniel, D.K., and Hanson, G.N., 1993, Geochemical approaches to sedimentation, provenance, and tectonics, *in* Johnson, M.J., and Basu, A., eds., Processes controlling the composition of clastic sediments: Boulder, Colorado, Geological Society of America Special Paper 284, p. 21–40.

Metcalf, R.V., Wallin, E.T., Willse, K.R., and Muller, E.R., 2000, Geology and geochemistry of the ophiolitic Trinity terrane, California; Evidence of middle Paleozoic depleted supra-subduction zone magmatism in a proto-arc setting, *in* Dilek, Y., et al., Ophiolites and oceanic crust; New insights from field studies and the Ocean Drilling Program: Boulder, Colorado, Geological Society of America Special Paper 349, p. 403–418.

Miller, M.M., and Saleeby, J.B., 1995, U-Pb geochronology of detrital zircon from Upper Jurassic synorogenic turbidites, Galice Formation, and related rocks, western Klamath Mountains; Correlation and Klamath Mountains provenance: Journal of Geophysical Research, v. 100, p. 18,045–18,058, doi: 10.1029/95JB00761.

Miller, J.S., Miller, R.B., Wooden, J.L., and Harper, G.D., 2003, Geochronologic links between the Ingalls Ophiolite, North Cascades, Washington and the Josephine Ophiolite, Klamath Mts., Oregon and California: Geological Society of America Abstracts with Programs, v. 35, no. 6, p. 113.

Miller, R.B., Mattinson, J.M., Funk, S.G., Hopson, C.A., and Treat, C.L., 1993, Tectonic evolution of Mesozoic rocks in the southern and central Washington Cascades, *in* Dunn, G., and McDougall, K., eds., Mesozoic Paleogeography of the western United States—II: Los Angeles, Pacific Section, Society of Economic Paleontologists and Mineralogists, v. 71, p. 81–98.

Norman, E.A.S., 1984, The structure and petrology of the Summit Valley area, Klamath Mountains, California [M.S. thesis]: Salt Lake City, University of Utah, 148 p.

Ohr, M., 1987, Geology, geochemistry, and geochronology of the Lems Ridge olistostrome, Klamath Mountains, California [M.S. thesis]: Albany, State University of New York, 247 p.

Park-Jones, R., 1988, Sedimentology, structure, and geochemistry of the Galice Formation: Sediment fill of a back-arc basin and island arc in the western Klamath Mountains [M.S. thesis]: Albany, State University of New York, 165 p.

Parkinson, I.J., and Pearce, J.A., 1998, Peridotites from the Izu-Bonin-Mariana forearc (ODP Leg 125); Evidence for mantle melting and melt-mantle interaction in a supra-subduction zone setting: Journal of Petrology, v. 39, p. 1577–1618, doi: 10.1093/petrology/39.9.1577.

Parson, L.M., and Wright, I.C., 1996, The Lau-Hauvre-Taupo back-arc basin: A southward-propagating, multi-stage evolution from rifting to spreading: Tectonophysics, v. 263, p. 1–22, doi: 10.1016/S0040-1951(96)00029-7.

Pearce, J.A., Baker, P.E., Harvey, P.K., and Luff, I.W., 1995, Geochemical evidence for subduction fluxes, mantle melting and fractional crystallization beneath the South Sandwich island arc: Journal of Petrology, v. 36, p. 1073–1109.

Pessagno, E.A., Jr., and Blome, C.D., 1990, Implications of new Jurassic stratigraphic, geochronometric, and paleolatitudinal data from the Western Klamath terrane (Smith River and Rogue Valley subterranes): Geology, v. 18, p. 665–668.

Pessagno, E.A., Jr., and Whalen, P.A., 1982, Lower and Middle Jurassic Radiolaria (multicyrtid Nassellariina) from California, east-central Oregon and the Queen Charlotte Islands, B.C.: Micropaleontology, v. 28, p. 111–169.

Pessagno, E.A., Jr., Blome, C.D., Hull, D., and Six, W.M., Jr., 1993, Middle and Upper Jurassic radiolaria from the western Klamath terrane, Smith River subterrane, northwestern California: Their biostratigraphic, chronostratigraphic, geochronologic, and paleolatitudinal significance: Micropaleontology, v. 39, p. 93–166.

Pessagno, E.A., Jr., Hull, D.M., and Hopson, C.A., 2000, Tectonostratigraphic significance of sedimentary strata occurring within and above the Coast Range Ophiolite (California Coast Ranges) and the Josephine Ophiolite (Klamath Mountains), northwestern California, *in* Dilek, Y., et al., eds., Ophiolites and oceanic crust; New insights from field studies and the Ocean Drilling Program: Boulder, Colorado, Geological Society of America Special Paper 349, p. 383–394.

Pinto-Auso, M., and Harper, G.D., 1985, Sedimentation, metallogenesis, and

tectonic origin of the basal Galice Formation overlying the Josephine ophiolite, northwestern California: Journal of Geology, v. 93, p. 713–725.

Quick, J.E., 1981, Petrology and petrogenesis of the Trinity Peridotite, an upper mantle diapir in the eastern Klamath Mountains, northern California: Journal of Geophysical Research, v. 86, p. 11,837–11,863.

Ravizza, G., Sherrell, R.M., Field, M.P., and Pickett, E.A., 1999, Geochemistry of the Margi umbers, Cyprus, and the Os isotope composition of Cretaceous seawater: Geology, v. 27, p. 971–974, doi: 10.1130/0091-7613(1999)027<0971:GOTMUC>2.3.CO;2.

Renne, P.R., and Scott, G.R., 1986, Paleomagnetism of the Upper Jurassic Galice Formation, southwestern Oregon: Evidence for differential rotation of the eastern and western Klamath Mountains: Comment: Geology, v. 14, p. 1048–1049, doi: 10.1130/0091-7613(1986)14<1048:CAROPO>2.0.CO;2.

Renne, P.R., and Scott, G.R., 1988, Structural chronology, oroclinal deformation, and tectonic evolution of the southeastern Klamath Mountains, California: Tectonics, v. 7, p. 1223–1242.

Roser, B.P., and Korsch, R.J., 1986, Determination of tectonic setting of sandstone-mudstone suites using SiO_2 content and K_2O/Na_2O ratios: Journal of Geology, v. 94, p. 635–650.

Roser, B.P., and Korsch, R.J., 1988, Provenance signatures of sandstone-mudstone suites determined using discriminant function analysis of major-element data: Chemical Geology, v. 67, p. 119–139, doi: 10.1016/0009-2541(88)90010-1.

Rowley, D.B., and Kidd, W.S.F., 1981, Stratigraphic relationships and detrital composition of the medial Ordovician flysch of western New England; Implications for the tectonic evolution of the Taconic Orogeny: Journal of Geology, v. 89, p. 199–218.

Saleeby, J.B., 1984, Pb/U zircon ages from the Rogue River area, western Jurassic belt Klamath Mountains, Oregon: Geological Society of America Abstracts with Programs, v. 16, p. 331.

Saleeby, J.B., and Busby-Spera, C., 1992, Early Mesozoic tectonic evolution of the western U.S. Cordillera, *in* Burchfiel, B.C., Lipman, P.W., and Zoback, M.L., eds., The Cordilleran Orogen; Conterminous U.S.: Boulder, Colorado, Geological Society of America, The Geology of North America, v. G-3, p. 107–168.

Saleeby, J.B., and Harper, G.D., 1993, Tectonic relations between the Galice Formation and the Condrey Mountain Schist, Klamath Mountains, northern California, *in* Dunn, G.C., and McDougall, K.A., eds., Mesozoic Paleogeography of the western United States—II: Los Angeles, Pacific Section, Society of Economic Paleontologists and Mineralogists, v. 71, p. 61–80.

Saleeby, J.B., Harper, G.D., Snoke, A.W., and Sharp, W., 1982, Time relations and structural-stratigraphic patterns in ophiolite accretion, west-central Klamath Mountains, California: Journal of Geophysical Research, v. 87, p. 3831–3848.

Saunders, A.D., and Tarney, J., 1979, The geochemistry of basalts from a back-arc spreading centre in the East Scotia Sea: Geochimica et Cosmochimica Acta, v. 43, p. 555–572, doi: 10.1016/0016-7037(79)90165-0.

Schultz, K.L., and Levi, S., 1983, Paleomagnetism of middle Jurassic plutons of the north-central Klamath Mountains: Geological Society of America Abstracts with Programs, v. 15, p. 427.

Seiders, V.M., 1991, Conglomerate stratigraphy and tectonics in the Franciscan assemblage of northern California and implications for Cordilleran tectonics: Reston, Virginia, U.S. Geological Survey Open-File Report PFR 91–50, 10 p.

Seiders, V.M., and Blome, C.D., 1988, Implications of upper Mesozoic conglomerate for suspect terrane in western California and adjacent areas: Geological Society of America Bulletin, v. 100, p. 374–391, doi: 10.1130/0016-7606(1988)100<0374:IOUMCF>2.3.CO;2.

Smith, G.M., and Harper, G.D., 1993, Paleomagnetism of the Josephine ophiolite: EOS, Transactions, American Geophysical Union, v. 74, p. 214.

Snoke, A.W., 1972, The petrology and structure of the Preston Peak area, Del Norte and Siskiyou counties, California [Ph.D. dissertation]: Stanford, California, Stanford University, 274 p.

Snoke, A.W., 1977, A thrust plate of ophiolitic rocks in the Preston Peak area, Klamath Mountains, California: Geological Society of America Bulletin, v. 88, p. 1641–1659, doi: 10.1130/0016-7606(1977)88<1641:ATPOOR>2.0.CO;2.

Southwick, D.L., 1974, Geology of the alpine-type ultramafic complex near Mount Stuart, Washington: Geological Society of America Bulletin, v. 85, p. 391–402, doi: 10.1130/0016-7606(1974)85<391:GOTAUC>2.0.CO;2.

Umino, S., 1986, Magma mixing in boninite sequence of Chichijima, Bonin Islands: Journal of Volcanology and Geothermal Research, v. 29, p. 125–157, doi: 10.1016/0377-0273(86)90042-9.

Vail, S.G., 1977, Geology and geochemistry of the Oregon Mountain area, southwest Oregon and northern California [Ph.D. dissertation]: Corvallis, Oregon State University, 159 p.

Wells, F.G., and Walker, G.W., 1953, Geology of the Galice quadrangle, Oregon: Washington, D.C., U.S. Geological Survey Geological Quadrangle Map GQ-25, scale 1:62,500, 1 sheet.

Wells, F.G., Hotz, P.E., and Cater, F.W., 1949, Preliminary description of the geology of the Kerby quadrangle: Portland, Oregon Department of Geology and Mineral Industries Bulletin, v. 40, 23 p.

Wright, J.E., 1982, Permo-Triassic accretionary subduction complex, southwestern Klamath Mountains, northern California: Journal of Geophysical Research, v. 87, p. 3805–3818.

Wright, J.E., and Fahan, M.R., 1988, An expanded view of Jurassic orogenesis in the western United States Cordillera: Middle Jurassic (pre-Nevadan) regional metamorphism and thrust faulting within an active arc environment, Klamath Mountains, California: Geological Society of America Bulletin, v. 100, p. 859–876, doi: 10.1130/0016-7606(1988)100<0859:AEVOJO>2.3.CO;2.

Wright, J.E., and Wyld, S.J., 1994, The Rattlesnake Creek terrane, Klamath Mountains, California: An early Mesozoic volcanic arc and its basement of tectonically disrupted oceanic crust: Geological Society of America Bulletin, v. 106, p. 1033–1056, doi: 10.1130/0016-7606(1994)106<1033:TRCTKM>2.3.CO;2.

Wyld, S.J., 1985, Geology of the western Jurassic Belt, South Fork Trinity River Area, Klamath Mountains, California [M.S. thesis]: Berkeley, University of California, 168 p.

Wyld, S.J., and Wright, J.E., 1988, The Devils Elbow ophiolite remnant and overlying Galice Formation: New constraints on the Middle to Late Jurassic evolution of the Klamath Mountains, California: Geological Society of America Bulletin, v. 100, p. 29–44, doi: 10.1130/0016-7606(1988)100<0029:TDEORA>2.3.CO;2.

Wyld, S.J., and Wright, J.E., 2001, New evidence for Cretaceous strike-slip faulting in the United States Cordillera and implications for terrane-displacement, deformation patterns, and plutonism: American Journal of Science, v. 301, p. 150–181.

Yule, J.D., 1996, Geologic and tectonic evolution of Jurassic marginal ocean basin lithosphere, Klamath Mountains, Oregon [Ph.D. dissertation]: Pasadena, California Institute of Technology, 308 p.

Yule, J.D., Saleeby, J.B., and Barnes, C.G., 1996, The 175–135 Ma plutons of the Klamath Mountains province reinterpreted as a single oceanic arc batholithic system: Geological Society of America Abstracts with Programs, v. 28, no. 5, p. 128.

Yule, J.D., Saleeby, J.B., and Barnes, C.G., 2006, this volume, A rift-edge facies of the Late Jurassic Rogue–Chetco arc and Josephine ophiolite, Klamath Mountains, Oregon, *in* Snoke, A.W., and Barnes, C.G., eds., Geological studies in the Klamath Mountains province, California and Oregon: A volume in honor of William P. Irwin: Boulder, Colorado, Geological Society of America Special Paper 410, doi: 10.1130/2006.2410(03).

Zierenberg, R.A., Shanks, W.C., III, Seyfried, W.E., Jr., Koski, R.A., and Strickler, M.D., 1988, Mineralization, alteration, and hydrothermal metamorphism of the ophiolite-hosted Turner-Albright sulfide deposit, southwestern Oregon: Journal of Geophysical Research, v. 93, p. 4657–4674.

Manuscript Accepted by the Society 10 January 2006

Printed in the USA